Investment in wind-based hydrogen production under economic and physical uncertainties

Luis Mª Abadie [a,c], José M. Chamorro [b,*]

[a] *Basque Centre for Climate Change (BC3), Sede Building 1, 1st floor, Scientific Campus, University of the Basque Country UPV/EHU, 48940 Leioa, Spain*
[b] *Dpt. Financial Economics II and Institute of Public Economics, University of the Basque Country UPV/EHU, Av. Lehendakari Aguirre 83, 48015 Bilbao, Spain*
[c] *Metroeconomica, Av. Zugazarte 8, 3rd floor (modules 5&6), 48930 Areeta, Spain*

HIGHLIGHTS

- This paper evaluates a wind farm that feeds a electrlolyzer for producing hydrogen.
- Both the spot power price and the wind capacity factor follow stochastic processes.
- These processes show distinctive seasonalities along with mean reversion and jumps.
- The paper uses Spanish data for parameter estimation, simulation and optimization.
- Green hydrogen turns economically viable above 3 €/kg. Sensitivity analyses follow.

ARTICLE INFO

ABSTRACT

This paper evaluates the economic viability of a combined wind-based green-hydrogen facility from an investor's viewpoint. The paper introduces a theoretical model and demonstrates it by example. The valuation model assumes that both the spot price of electricity and wind capacity factor evolve stochastically over time; these state variables can in principle be correlated. Besides, it explicitly considers the possibility to use curtailed wind energy for producing hydrogen. The model derives the investment project's net present value (NPV) as a function of hydrogen price and conversion capacity. Thus, the NPV is computed for a given price and a range of capacities. The one that leads to the maximum NPV is the 'optimal' capacity (for the given price). Next, the authors estimate the parameters underlying the two stochastic processes from Spanish hourly data. These numerical estimates allow simulate hourly paths of both variables over the facility's expected useful lifetime (30 years). According to the results, green hydrogen production starts becoming economically viable above 3 €/kg. Besides, it takes a hydrogen price of 4.7 €/kg to reach an optimal conversion capacity half the capacity of the wind park. The authors develop sensitivity analyses with respect to wind capacity factor, curtailment rate, and discount rate.

1. Introduction.

The 2015 Paris Climate Agreement aims to limit global warming this century to well below 2 degrees Celsius (preferably 1.5) compared to pre-industrial levels. This long-term goal puts pressure on signatory countries to achieve climate neutrality by mid-century. In response, every-five years they submit their intended climate policies (the so-called nationally determined-contributions, NDCs). After two successive rounds of NDC pledges, the countries at the UN climate conference in Glasgow 2021 (COP26) committed to reducing 6.3 billion tonnes of greenhouse gas (GHG) emissions by 2030. This challenge in turn calls for

transforming current production and consumption patterns, and shifting toward a circular economy. Energy supply is a priority sector in this regard. The share of electricity in particular is forecasted to increase sharply in the future; IEA [1].

Power generation can be decarbonized by using energy sources with low or no GHG emissions attached. Variable renewable energy (VRE) resources such as solar and wind belong in this family. Unfortunately, however, they are intermittent and uncertain. They strongly depend on local weather conditions, which are rather different across space and time. These characteristics complicate the engineering and the economics of harnessing them for power generation. Sinsel *et al.* [2] provide an overview of the challenges created by variable renewables and the

Nomenclature

(i=Electricity spot price E;wind capacity factor (CF)

β_1^i	Constant	FC^e	Wind energy fixed operating costs
β_2^i	Deterministic trend	FC^h	PtG fixed operating costs
$\beta_3^i - \beta_{12}^i$	Yearly cycle parameters	p_t^e	Electricity price in hour t
$\beta_{13}^i - \beta_{18}^i$	Weekly cycle parameters	CF_t	Wind capacity factor in hour t
$\beta_{19}^i - \beta_{28}^i$	Daily cycle parameters	p_t^h	Hydrogen price in hour t
α^i	Numerator of long run mean (α/κ)	MW	Megawatt
κ^i	Rate of reversion toward mean	MWh	Megawatt-hour
μ_j^i	Mean jump	CM	Contribution margin (€)
σ^i	Volatility of mean-reverting part	k_h	PtG capacity relative to wind farm capacity
σ_j^i	Volatility of jump part	k_e	Wind farm capacity (assumed 1 MW)
λ^i	Jump probability	TX	Present value of corporate income taxes
ρ	Correlation coefficient	η	Conversion rate
γ	Degradation rate	SP^e	Wind power technology's cost
d^n	Depreciation factor	SP^h	Power to Gas (PtG) system price
w^e	Wind energy variable operating cost	φ	Unused share
w^h	PtG variable operating cost	r	Discount rate (WACC, real)
		r_f	Risk-free rate
		T	Useful lifetime
		α	Income tax rate
		NPV	Net Present Value

solution technologies available for addressing them. They find that flexibility technologies dominate grid technologies in terms of solution potential.

Now, hydrogen shows considerable potential on both accounts: abatement of GHG emissions and penetration of VRE resources. On one hand, unlike fossil fuels it contains no carbon. Yet, just as them, it lends itself to a range of applications, e.g. in transportation, manufacturing, heat and power generation… Nonetheless, hydrogen is not a source of primary energy. It is an energy carrier: it requires a prior energy input to be produced; Nikolaidis and Poullikkas [3] provide a comparative overview of the main hydrogen production processes. Besides, hydrogen is able to store energy to be released gradually when required. Indeed, these special features render it a suitable complement to power supply from VRE resources like wind and solar. These sites can make use of surplus generation (thus decreasing curtailment) to produce hydrogen, which in turn allows reducing optimal VRE capacity investment; Stöckl *et al.* [4]. It is possible to exploit these synergies by combining an investment in a VRE facility with a power-to-gas (PtG) facility. The first PtG system for this purpose was realized in 1991, though it is in the 21st century when the number of facilities has taken off. Gahleitner [5] reviews 41 realized projects between 1990 and 2012 and seven planned projects at the time.

This combined system provides flexibility in three important dimensions (Jaunatre [6]): (i) Time: the firm decides the optimal time to switch from one use (produce electricity for sale) to another (produce hydrogen instead), depending on their relative prices. (ii) Location: existing pipelines and shipping lines can transport energy in a chemical form (H_2) thus replacing costly infrastructures for transporting electricity. The former system not only reduces losses along the transportation process; it enables providing end-users located far away from VRE generation places with VRE as well. (iii) End use ('sector coupling'): by changing the energy vector, otherwise hard-to-electrify sectors (e.g. industry, transport, buildings heating and cooling) can use VRE. Integrating these energy-consuming sectors with the power generation sector smooths fluctuations and reduces the need for electricity and CO2 storages. Consequently, the energy system's costs decrease and a larger share of VRE can be used; Schultes and Madlener [7]. They can use hydrogen as such (i.e. in fuel cells) or transform it into another substance (e.g. ammonia, methanol).

The focus here falls on the first option: at any time, the manager of the wind power plant must choose between selling the power produced at the current price in the electricity market or, alternatively, feeding it to the electrolyzer for converting it into hydrogen. Thus, the authors address the valuation of the combined system. This is different from valuing the opportunity to invest in that system. Clearly, as the system's profitability increases, the option to invest in it becomes more valuable. In options language, the system is the 'underlying asset' and the opportunity to invest in it is the 'derivative asset'. Potential investors in such a system have other 'real options' at their disposal, e.g. the option to delay investment, to modify the scale of the project, to close down temporarily, or to abandon it. The authors leave these real options aside.

The authors adopt the viewpoint of a potential investor assessing a combined system like the above one from a financial perspective. Following Glenk and Reichelstein [8], the authors consider a polymer electrolyte membrane (PEM) electrolyzer. Although its CAPEX and operating costs are higher than those of alkaline electrolysis cells, PEM technology seems to be the leading technology because of its high efficiency and superior compatibility with the changing power produced from VREs; Shaner *et al.* [9], Jaunatre [5]. It is safe and reliable, and has good lifetime characteristics; Way *et al.* [10]. Besides, PEM-based hydrogen can be directly stored or linked to a pipeline due to its pressure; Touili *et al.* [11]. The authors assume that the system size is 'small', so it has no significant impact on electricity and hydrogen prices. The main investment criterion here is the Net Present Value (NPV) under uncertainty, i.e. the difference between the present value (PV) of expected cash inflows and that of expected outflows. Computing the project NPV directly addresses the first question, namely whether the project is profitable or not under current circumstances. Nonetheless, a point estimate of the NPV is hardly enough. Sensible investors do not consider a single scenario nor a handful of possible scenarios, the less so when, as in this case, some state variables are correlated. So, what could happen with the project when considering a large number of possible scenarios? To this end, the authors run Monte Carlo simulation (Section 5); the resulting distribution of project outcomes sheds much more information on the system profitability than the point-estimate NPV. At the same time, sensible investors try to pinpoint the crucial assumptions behind the project NPV. Thus, the third question is: what are the consequences of changes (or forecast errors) in the key project variables on the NPV? Following standard practice, the authors address it by means of sensitivity analysis (Section 6).

1.1. Overview of the related literature.

Van Benthem *et al.* [12] propose an options model to compute the value and timing strategy of an investment in a hydrogen infrastructure. With Japan in mind, a firm engages simultaneously in producing hydrogen from natural gas (via steam methane reforming, SMR, with carbon capture) and selling it in the retail market to drivers of fuel-cell vehicles (FCVs) which it also produces. Guerra *et al.* [13] look instead at the cost of producing hydrogen from the power grid via electrolysis. Given the major impact of power prices on this cost, they consider about 7,200 industrial and commercial US retail rates. They find hydrogen production costs below 4$/kg in 20 us states (which makes hydrogen cost-competitive with gasoline and diesel vehicle fuel costs at some places). Stöckl *et al.* [4] too focus on how to decarbonize road-based passenger transportation in Germany, in this case by means of green hydrogen. Specifically, they use an open-source co-optimization model that minimizes the total system costs of providing electricity and electrolysis-based hydrogen at filling stations while explicitly considering how green hydrogen interacts with the power sector. Talebian *et al.* [14] analyze the best support measures for easing the deployment of a green hydrogen supply chain aiming at light-duty passenger vehicles in British Columbia. Coppitters *et al.* [15] consider a wind-and-solar-powered hydrogen refueling station for a bus fleet in Belgium.

Hydrogen can be put to other uses. Ishaq *et al.* [16] analyze a co-generation system that integrates a wind turbine with an electrolyzer and a fuel cell to provide both electricity and heat to a community of 25 households. Farhat and Reichelstein [17] consider a polygeneration energy system (PES) that uses fossil fuels (coal and petcoke) as inputs and produces hydrogen as an intermediate product. The latter is either fed into a combined-cycle turbine unit for electricity generation or mixed with nitrogen to produce ammonia, the precursor material for making fertilizers (e.g. urea). They examine the economic competitiveness of a PES system in California. Klyapovskiy *et al.* [18] consider a system in Denmark where hydrogen is produced from renewable energy, and account for the flexibility provided by industrial plants via conventional demand response and Power-to-X capabilities (where X can denote ammonia, hydrogen, synthetic gases or liquid fuels).

Closer to this paper, Kroniger and Madlener [19] evaluate the option to enhance a wind farm with an electrolyzer that uses excess electricity to produce hydrogen, which is then compressed and stored ('power to gas'). With this upgrade, even if the wind farm is disconnected from the grid it can still operate, thus increasing its utilization rate. In addition, a fuel cell (or novel hydrogen gas turbine) is attached, so it can also engage in temporal arbitrage, purchasing power at low spot market prices to produce hydrogen and then re-electrifying at times of high prices. They develop a stochastic model that accounts for uncertain wind speed, spot market prices, and call of minute reserve capacity. These fluctuating input parameters are simulated via Monte Carlo. They result into stochastic cash flows and hence hourly profits, which are assumed to follow a geometric Brownian motion. Grueger *et al.* [20] similarly address the combination of wind farms with electrolyzers ('power to gas') and fuel cells ('re-electrification'). These flexible combined systems can in principle accommodate and/or reduce wind farm forecast errors and increase the system's ability to provide secondary control reserve. Another double-way system is considered by Eypasch *et al.* [21]. Specifically, a stationary electricity storage system must meet demand in an industrial plant without disruption. Both wind farms and PV panels supply the electricity (supplemented from the power grid if necessary). Unlike previous papers, hydrogen is chemically stored in Liquid Organic Hydrogen Carriers, which is convenient for safe and lossless storage of hydrogen over long periods. Glenk and Reichelstein [8] develop an analytical framework that applies to general hybrid energy systems and yields necessary and sufficient conditions for their economic viability. The model includes an adjustment factor that accounts for covariances between renewable power generation (via capacity factor, i.e. the ratio between its actual power production and maximum possible production) and power market prices.

1.2. Contribution.

It is possible to identify some shortcomings in the related literature, e.g. a time horizon of a single year, deterministic (even fixed) commodity prices, wind capacity factor running at its average value… In other instances, these variables are uncertain but the stochastic processes adopted are unable to account for the complex dynamics underlying them. Sometimes optimization and/or simulation play only a limited role in the empirical applications.

This paper contributes to this literature on several grounds. A major contribution is that both the electricity spot price and the wind capacity factor behave stochastically over time; see for example Abadie and Chamorro [22]. There is room for several seasonal patterns overlapping with mean reversion, continuous shocks, and discrete jumps. The model allows for the possibility that these variables are correlated. The authors propose specific stochastic processes for them, which comprise a deterministic part and a stochastic part. Later on, they estimate the underlying parameters of the two stochastic processes from (Spanish) official or publicly available data sources; this is another major contribution. The numerical estimates are then embedded into a valuation model that takes the expected system lifetime (30 years) into account on an hourly basis. Similarly relevant is a lower usage of formulas, the solution by Monte Carlo simulation (10,000 runs), determination of the optimal operation mode, and the corresponding optimal conversion capacity under uncertainty. This in turn allows derivation of the expected NPV (and the probability distribution). A minor contribution is a different, more realistic specification of the corporate income tax.

Section 2 introduces the valuation model. Section 3 provides some background on the data sample as a prior step toward parameter estimation and model simulation. Section 4 shows the empirical results in the base case. The information about the project NPV goes along with that on the optimal hydrogen conversion capacity and hydrogen production. The authors undertake a few sensitivity analyses in Section 5. Concluding remarks are in Section 6.

2. Material and modelling.

The section comprises three parts. Since the valuation model is ultimately demonstrated by example, first there is a cursory look at the data to identify the most salient features that the model should account for. Next, this paper proposes a model for the stochastic behavior of the two sources of uncertainty. The electricity price and the capacity factor are assumed to behave in this particular way within the overall valuation model for the combined system in the third part. The latter draws on Glenk and Reichelstein [8] to some extent. Nonetheless, as mentioned earlier, there are several differences.

2.1. Background data.

In this paper there are two risk factors: a price (p_t^e) and a quantity (CF_t). In principle, it could be possible to blend them from the very beginning. For instance, Schultes and Madlener [7] consider the (quarterly) revenue flow as a state variable. However, the paper here deals with them separately and over short periods of time (namely, hours). This is one possible way to sidestep the problem addressed by Reichelstein and Sahoo [23]: failure to capture any synergies between the capacity factor and the electricity price will generally lead to biases in the traditional LCOE (or LCOH) calculation.

Our data include three sets of information, which can be downloaded from the publicly available database of the Spanish power transmission and distribution system operator, Red Eléctrica de España [24]:

Table 1
Descriptive statistics of hourly electricity price (p_t^e) and capacity factor (CF_t).

	Electricity Price (€/MWh)	Capacity Factor
Mean	49.214	0.2409
Minimum	0.03 (2016/01/19)	0.0051 (2019/10/21)
Maximum	101.99 (2017/01/25)	0.7587 (2016/01/11)
Standard Deviation	14.3450	0.1415
Skewness	−0.4534	0.7730
Excess Kurtosis	0.7700	0.0212
5 % Percentile	23.0320	0.0590
95 % Percentile	70.6700	0.5252

a) Spanish hourly spot electricity price (p_t^e) (in €/MWh) for the period 2016–2019, that is 35,064 hourly prices.
b) Hourly electricity generation from Spanish onshore wind farms (MWh) for the same period.
c) Monthly installed capacity (MW) of onshore wind farms from December 2015 to December 2019. The authors transform these monthly data into hourly data by linear interpolation.

Drawing on (b) and (c) the authors compute the hourly capacity Factor. See Table 1. The average CF is 24.09 %, with a minimum of 0.51

% and a maximum of 75.87 %. The 90 % confidence interval stretches from 5.90 % to 52.52 %. A number of Spanish wind farms are very old (up to 30 years), and they usually use wind turbines with low rated power. These facts quite possibly induce a downward bias on the average CF. To lessen this impact, in our calculations below (from Section 4.2.2. onwards) the authors apply a linear transformation to the original CF series. Specifically, the authors multiply the original numbers by a scalar, 0.38/0.2409, in order to raise the average to 38 % (more representative of recent parks, indeed the value for France, IEA [25] while keeping the stochastics of the original series intact.

Fig. 1 shows power price over the period 2016–2019. A sizeable volatility coexists with sudden spikes and seasonal features (e.g. the high levels around January).

Fig. 2 displays the evolution of the capacity factor; the underlying installed capacity of onshore wind farms can be found in APPENDIX B, Fig. B.1. Again the data show a high volatility along with abrupt swings and seasonal patterns. Under these circumstances day-ahead prediction is extremely prone to sizeable deviations from observed values; Han *et al.* [26]. Poor forecasting accuracy exacerbates the difficulty of keeping power balance within each period. The ensuing imbalances can lead to wind power curtailment (and/or load shedding). Similar wild patterns on an hourly basis for average days across the months of a year in
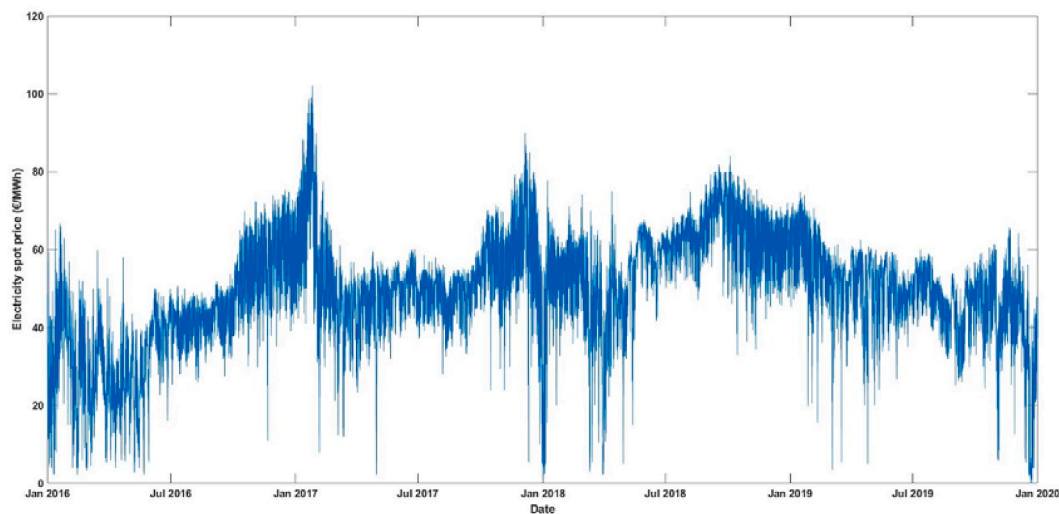

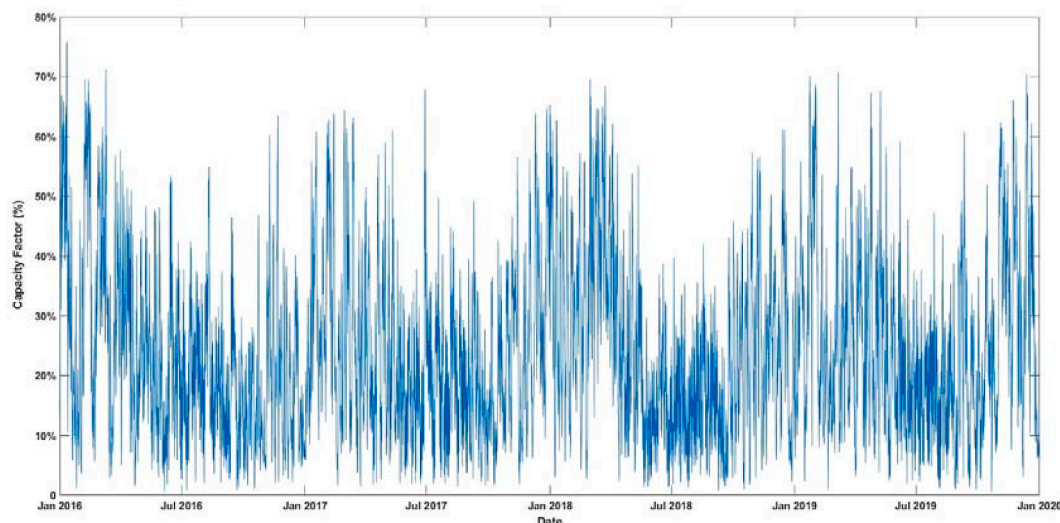**Fig. 1.** Hourly spot price of electricity in Spain, 2016–2019.

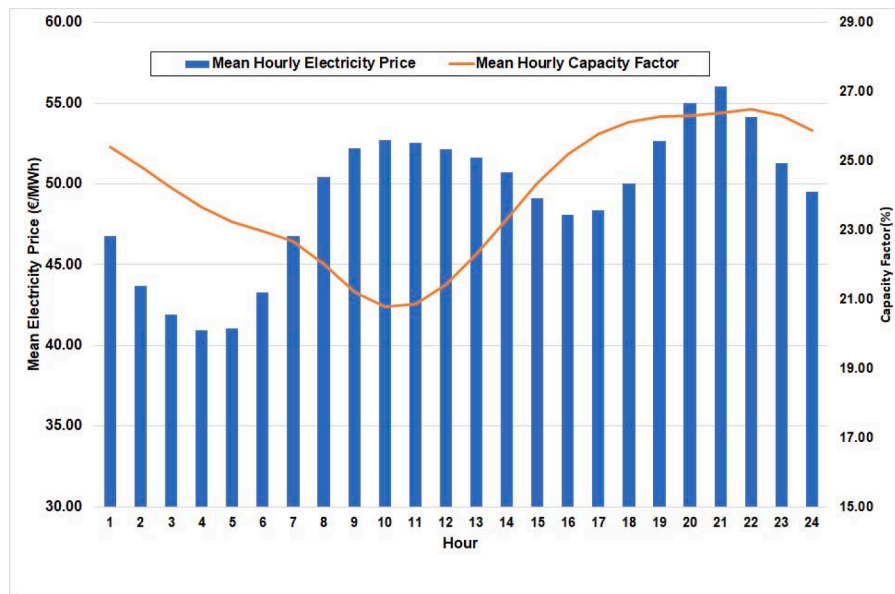**Fig. 2.** Hourly capacity factor in Spain, 2016–2019.

Fig. 3. Average capacity factor and power price in Spain, 2016–2019.

Toronto (Canada) can be found in Ishaq and Dincer [27].

Up to this point, the authors have looked at the data as a pair of two time series. Now the authors compute their average values over each of the 24 h of the day; see Fig. 3. Starting from 7:00 until 15:00 the power price is relatively high whereas the capacity factors is comparatively low. At other times, however, both decrease, or increase, or reach their maxima at about the same hour (20:00).

There are other places where wind speeds over the day and/or the year turn out to be correlated with the power system's load and wholesale price. Depending on its magnitude and sign, this correlation can make wind facilities at different locations either more or less valuable. Fripp and Wiser [28] address the issue across a broad geographical area in the U.S. west. According to their results, the timing of wind has a moderate impact on their financial value in the wholesale power market (up to 4 % higher than the average market price for the best-timed power sites). Nonetheless, it has a substantial impact on their capacity factor (those sites could produce up to 30 %-40 % more power during the top 10 % peak-load hours than their average over the year). Jørgensen and Ropenus [29] look at Danish data and also find an inverse relationship between the hourly wholesale price of power and the concurrent amount of wind generation.

Further, Reuter *et al.* [30] find that an investor in a wind power plant will get an expected profit that is higher with a constant load factor (23 %) than with a variable one (normally distributed around a mean of 23 % with a standard deviation of 6 %): "*this is caused by the link between aggregate supply and the electricity price*". Reichelstein and Sahoo [23] claim that, if the investor faces a price schedule that varies by time of day and possibly also by season, the failure to capture any synergies between the capacity factor and the electricity price will generally lead to biases in the calculation of life-cycle cost concepts (e.g. the levelized cost of electricity, LCOE, or hydrogen, LCOH). Nonetheless, they demonstrate that a levelized cost analysis remains appropriate for assessing the cost competitiveness of an intermittent power source, provided that the figure obtained from a traditional average LCOE calculation is adjusted by a multiplicative correction factor, which they term the 'co-variation coefficient'. Specifically, they estimate co-variation coefficients of 0.87 and 0.92 for wind generation sites near Livermore, CA and Benicia, CA, respectively. Similarly, Glenk and Reichelstein [8] claim that "*on the revenue side, the inherent intermittency of the renewable source and the continuous fluctuations in electricity prices demand to account for covariances between renewable power generation and*

market prices". Their numerical calculations include a 'co-variation coefficient' (namely 0.88) that "*captures the variation between output and price*".

2.2. Stochastic model for the risk factors.

This paper focuses on the valuation of an investment project under uncertainty. Maximizing its value (from an investor's viewpoint) draws on stochastic optimization methods. One of them is stochastic programming. In this approach, a huge number of different scenarios that comply with the probabilistic features of the uncertainties are considered. The value of the asset is optimized in each of these scenarios. Then, the average or expected value is calculated. There are other methods, among them robust optimization. This approach leads to optimized solutions under a single scenario, namely the worst-case scenario. Robust design optimization aims at optimizing both the expected value and the standard deviation; Coppitters *et al.* [15]. Unlike the former, data-driven robust optimization does not assume a particular probability distribution of the uncertain parameter(s). Instead, it draws on a so-called ambiguity set, which includes possible distributions. Zheng *et al.* [31] follow this approach to tackle uncertainties from both wind power and electricity price. The process is assisted by a multi-layer perception neural network.

The authors here stick to stochastic programming. Regarding long-term valuation of energy assets, commodity prices tend to revert toward levels of equilibrium after an incidental change. This paper introduces a stochastic process that allows for mean reversion and discrete jumps in addition to random shocks (whether continuous or otherwise). This flexible specification accounts for different variability structures. Besides, several price models typical in the commodities literature are nested in it (depending on the values adopted by the underlying parameters). These characteristics of generality and versatility lead us to assume the same process for the wind capacity factor.

The authors propose a common process, *T*, for both sources of risk, which comprises a deterministic part, *D*, and a stochastic part, *S*, while allowing for correlation between the two sources:

$$T_t^i = D^i(t) + S_t^i \tag{1}$$

where $i = \{E, CF\}$.

By assumption, the mathematical expectation of the stochastic part S^i is zero. This suggests mean reversion over time; nonetheless, the mean

level is going to change with the passage of time. Therefore, when it comes to forecasting, only D^i is relevant:

$$D^i(t) = \beta_1^i + \beta_2^i t + YC^i(t) + WC^i(t) + DC^i(t) \tag{2}$$

Time (t) will be measured in years on an hourly basis. For instance, the first hour in 2016 is $t = 1/366/24$ because 2016 was a leap year; the first one in 2017 is $t = 1 + (1/365/24)$. In addition to a constant, β_1^i, and a time trend, $\beta_2^i t$, the model for D^i includes:

a) **A yearly cycle**, $YC^i(t)$: it encompasses different seasonal components (annual, semi-annual, quarterly, semi-quarterly, …), as many as determined by statistical significance:

$$YC^i(t) = \sum_{j=1}^{5} [\beta_{1+2j}^i \sin(2j\pi t) + \beta_{2+2j}^i \cos(2j\pi t)] \tag{3}$$

Eq. (3) represents the yearly cycle with up to five sine and cosine components. If a specific coefficient turns out to be statistically non-significant (at standard confidence levels) in the estimation process it will be dropped. A number of model specifications and elimination procedures are available; see, for instance, Çanakoğlu and Adiyeke [32].

b) **A weekly cycle**, $WC^i(t)$, according to the day of the week:

$$WC^i(t) = \beta_{13}^i D_1(t) + \beta_{14}^i D_2(t) + \beta_{15}^i D_3(t) + \beta_{16}^i D_4(t) + \beta_{17}^i D_5(t) + \beta_{18}^i D_6(t) \tag{4}$$

In Eq. (4) there are six dummy variables. $D_1(t)$ equals 1 if it is Monday, and zero otherwise. $D_2(t) = 1$ on Tuesdays, and zero otherwise; and so on for the six dummy variables. When the six dummies are zero it is Sunday.

c) **A daily cycle**, $DC^i(t)$, based on the particular hours, with their own seasonalities:

$$DC^i(t) = \sum_{j=1}^{5} [\beta_{17+2j}^i \sin(2j\pi\tau)/24 + \beta_{18+2j}^i \cos(2i\pi\tau)/24] \tag{5}$$

Eq. (5) represents the daily cycle in hours. The index τ indicates the hour: $\tau = 1, 2,…, 24$.

In principle, there are 28 parameters in the deterministic part. As mentioned above, if any of them is not significant it will be eliminated, in which case the model is re-estimated again with less parameters.

On the other hand, the stochastic part, S_t^i, follows a continuous mean-reverting process with discrete jumps:

$$dS_t^E = (\alpha^E - \kappa^E S_t^E)dt + \sigma^E dW_t^E + J^E(\mu_j^E, \sigma_j^E)dq_j^E \tag{6}$$

$$dS_t^{CF} = (\alpha^{CF} - \kappa^{CF} S_t^{CF})dt + \sigma^{CF} dW_t^{CF} + J^{CF}(\mu_j^{CF}, \sigma_j^{CF})dq_j^{CF} \tag{7}$$

$$E(dW_t^E dW_t^{CF}) = \rho dt \tag{8}$$

Specifically, Equations (6)-(7) comprise three terms on the right hand. The first two of them constitute a so-called Ornstein-Uhlenbeck (OU) process; the third one is a Poisson process. Now, proceeding step by step in Eq. (14), the first term is a function of S_t^E, while the other two are stochastic. Leaving the latter aside for a moment, the equation can be rewritten as $dS_t^E = (\alpha^E - \kappa^E S_t^E)dt = \kappa^E(\frac{\alpha^E}{\kappa^E} - S_t^E)dt$. Thus, the stochastic part of the electricity price tends toward α^E/κ^E in the long term, with a reversion speed κ^E. If S_t^E falls below its long-run quilibrium level the parenthesis will be positive, which induces an increase in its value ($dS_t^E > 0$); and conversely: if S_t^E rises above α^E/κ^E the parenthesis will be negative, pushing S_t^E downwards ($dS_t^E < 0$). In sum, when S_t^E departs from its long-term equilibrium (due to the impact of stochastic shocks, namely OU and jumps), the first term tends to restore the equilibrium (always subject to shocks). Besides, the higher the speed of reversion κ^E, the sooner S_t^E approaches its equlibrium value. Now, the second term generates a continuous random behaviour (without jumps): the volatility of the mean-reverting process is σ^i; dW_t^i is the increment to a

standard Wiener process. The third term accounts for jumps in the electricity price with intensity λ^E (the mean rate of event occurrence); thus, if time is measured in years then λ^E jumps are expected per year. The jump size is normally distributed with mean μ_j^E and volatility σ_j^E. Here dq_j^E is a Poisson process such that $dq_j^E = 1$ with probability $\lambda^E dt$, and $dq_j^E = 0$ with probability $1 - \lambda^E dt$. The authors assume that dW_t^E and dq_j^E are independent. The same interpretation applies to Eq. (15) for the capacity factor.

On the other hand, sometimes the power price and the capacity factor can move stochastically for common reasons. Equation (8) shows that these processes are correlated as measured by ρ. In principle one would anticipate that increases in supply will push the price downward (and conversely), i.e. a negative correlation.

2.3. Model for the NPV of a green-hydrogen project.

Glenk and Reichelstein [8] derive the expression for the NPV of a hybrid system with a VRE normalized capacity of $k_e = 1$ kW and a PtG capacity of k_h^* (also measured in kW) which is to be optimally chosen (efficiently sized); that is, they compute the NPV of an optimized hybrid system, NPV(1, k_h^*). This system will be economically viable if its NPV is positive and higher than that of the renewable power system without PtG, i.e. NPV(1, 0), provided the latter is cost-competitive on its own:

$$NPV(1, k_h^*) \rangle \max[NPV(1,0); 0]. \tag{9}$$

The lowest hydrogen price for which the combined system makes economic sense (i.e. the above inequality applies) is the break-even price of hydrogen, p_h^*, which has a corresponding optimal PtG capacity k_h^* attached. They consider a time horizon of 1 year with hourly time steps and deterministic electricity price and capacity factor.

The approach that the authors follow here for deriving the NPV is: NPV = PV(Pre-tax net cash flows) — PV(Income taxes) — PV(Investment costs) (10).

The building blocks in our valuation framework are hourly cash flows. They start at the first hour of useful lifetime and run until the facility's maturity at the end of year T:

$$V_0 = \sum_{t=1}^{8760 \times T} CM_t e^{-(r+\gamma)t/8760} - T \times (FC^e + k_h \times FC^h) \tag{11}$$

Here T is the expected lifetime of the hybrid system (the same for both the wind park and the electrolyzer). FC^e and FC^h denote the yearly fixed operating cost per capacity unit of the renewable power station and the PtG facility, respectively; for simplicity, both are assumed to grow at the same rate as the discount rate r (cost of capital). Instead, the contribution margin CM of the hybrid system is subject to both degradation at a rate γ and discount (back to the present) at the rate r. Here degradation affects the hybrid system's contribution margin CM in monetary units. This is unlike Glenk and Reichelstein [8], where degradation impacts the system as such: a fraction of the capacity is lost in each subsequent year. Staffell and Green [33] look at UK's 282 onshore wind farms from 2002 to 2012 and find that wind turbines lose around 1.6 % of their output each year on average; they discuss several reasons for this decline. The authors assume that the wind plants are price takers in both the wholesale power market and the hydrogen market. k_h stands for the capacity of the PtG system relative to the wind farm's capacity, which is assumed to be $k_e = 1$ kW (nonetheless, the numerical results in Sections 4 and 5 assume $k_e = 1$ MW).

The contribution margin in hour t, with $t = 0, 1, 2,…, 8760 \times T$, is:

$$CM_t = p_t^e CF_t + \min(CF_t, k_h) \times \max(\eta(p_t^h - w^h) - p_t^e, 0) + \min(\varphi \times CF_t, k_h)\eta(p_t^h - w^h) \tag{12}$$

Where:

p_t^e is the electricity price in period t.

Table 2
Parameter estimates of the deterministic part of power price, $D^E(t)$. *.

Parameter	Coefficient	Std. Dev. **	t value	p value
Constant β_1	37.4135	0.9102	41.1000	<0.0001 ***
Trend β_2	2.8710	0.2894	9.9210	<0.0001 ***
YC β_3	−4.98833	0.3579	−13.94	<0.0001 ***
YC β_4	2.5441	0.4338	5.8650	<0.0001 ***
YC β_6	2.9652	0.4286	6.9180	<0.0001 ***
YC β_7	1.9372	0.3901	4.9660	<0.0001 ***
YC β_9	0.9340	0.4014	2.3270	0.02 **
YC β_{12}	−0.943505	0.4108	−2.297	0.0216 **
WC β_{13}	6.9148	0.8228	8.4040	<0.0001 ***
WC β_{14}	8.3514	0.9208	9.0690	<0.0001 ***
WC β_{15}	7.9039	0.9383	8.4230	<0.0001 ***
WC β_{16}	8.0250	0.9362	8.5710	<0.0001 ***
WC β_{17}	7.5614	0.9461	7.9920	<0.0001 ***
WC β_{18}	3.6903	0.8470	4.3570	<0.0001 ***
DC β_{19}	−3.55065	0.1013	−35.05	<0.0001 ***
DC β_{20}	−1.46278	0.0813	−18.00	<0.0001 ***
DC β_{21}	−4.15963	0.0754	−55.17	<0.0001 ***
DC β_{22}	1.9441	0.0527	36.8600	<0.0001 ***
DC β_{23}	−0.231774	0.0421	−5.506	<0.0001 ***
DC β_{24}	−0.0901982	0.0386	−2.335	0.0196 **
DC β_{25}	0.6183	0.0295	20.9400	<0.0001 ***
DC β_{26}	−0.558351	0.0280	−19.92	<0.0001 ***

  * Variables whose coefficients show statistical significance below 1% have been deleted.
  ** HAC standard deviations, with bandwidth 24 (Bartlett Kernel). Source: Authors calculations. Note: Asterisks denote statistical significance at levels:
  *** 0.1%; ** 1%.

p_t^h is the hydrogen price in period t.

CF_t is the capacity factor in period t. Depending on the institution collecting the data curtailment events may have been netted out previously (thus leading to a lower figure) or not.

η is the conversion rate of the electrolyzer, in kg H_2/kWh.

w^h is the variable cost per kg H_2. Steam methane reforming requires 4.5 kg of water per kg H_2 produced. Instead, water electrolysis takes about 10 kg H_2O per kg H_2; Mohsin et al. [34], Jaunatre [6].

φ is the unused share of the technical yield (e.g. because of curtailment); see APPENDIX A. Even when the grid operator complies with a mandate for preferential access to VREs, it is not possible to feed total wind energy into the grid all the time because of both local network and system-wide security issues, or negative residual load (Joos and Staffell [35]). Security-based limits lead to so-called 'curtailment'; Steurer et al. [36]. Sometimes there are technical reasons behind it. For one, high wind occurrence can give rise to grid overload and this in turn lead to grid instabilities; Kroniger and Madlener [19]. At the same time, curtailment does not preclude wind operators from providing upward reserves. Thus, under optimal dispatch, wind has a role not only as provider of energy, but flexibility and system services as well; Yasuda et al. [37]. On other occasions, the reasons behind curtailment are economical. As just mentioned, curtailing VRE allows to avoid operational costs for procuring systems reserve and regulating energy. Similarly, accommodating highly infrequent local and system-wide peaks in VRE feed-in would require costly investments in both grid and storage extension (in addition to their environmental implications). Yet, there are downsides to curtailment. The "missing" wind electricity under network congestion must be supplied somewhere else, e.g. conventional power plants, which has an impact on fuel consumption and the ensuing emissions. Bird et al. [38] identify a number of reasons for curtailment along with a variety of factors that affect the potential for curtailment.

As shown in Eq. (12), hourly CM_i comprises three items. The first one refers to wind electricity sold at the market price (note that the unit variable cost for the wind park is zero). At time t, at the very least, the firm will receive p_t^e times the capacity factor available at that time; this does not necessarily mean that electricity will be actually produced. Regarding the second term, if producing hydrogen is more profitable

than producing electricity then the firm will get an extra revenue worth the difference between both prices times the minimum of CF_t and k_h. The value of 1 kWh of electricity converted into hydrogen is $\eta(p_t^h - w^h)$, which is to be compared with its value without conversion (p_t^e); the maximum capacity is given by $\min(CF_t, k_h)$. Therefore, in this case of a positive price gap, if $CF_t > k_h$ then k_h sets the limit to hydrogen production (and $CF_t - k_h$ to power generation). This second term (the one in Glenk and Reichelstein [8]) encompasses the only two possible states: (i) when the park can feed its output into the power grid (and hence into the power market, so a choice between electricity and hydrogen must be made); (ii) when the output cannot be fed into the grid (for whatever reason, e.g. curtailment, so hydrogen is the only alternative). The authors separate both states in our model by adding a third term that explicitly accounts for state (ii). In other words, the third term shows the revenues from producing hydrogen with curtailed energy (i.e. energy that would never be used for power generation). Note that our CF data come from the power system operator, so presumably they are net of curtailment events. Thus, when wind power is curtailed the manager can seize upon the flexibility provided by the hybrid system: again, the conversion value of hydrogen $\eta(p_t^h - w^h)$ will be earned up to the maximum capacity available, in this case $\min(\varphi \times CF_t, k_h)$. We assume that all curtailed energy is used to produce hydrogen (up to the capacity limit).

Using hourly time steps over a 30-year useful lifetime Eq. (3) becomes:

$$V_0 = \sum_{t=1}^{8760 \times 30} CM_t e^{-(r+\gamma)t/8760} - 30 \times \left(FC^e + k_h \times FC^h\right) \tag{13}$$

Now, the taxable income in year n (with $n = 1, 2, \dots, T$) is:

$$TI_n = \sum_{t=1+8760(n-1)}^{8760 \times n} CM_t e^{-\gamma t/8760} - \left(FC^e + k_h \times FC^h\right)e^{rn} - \left(SP^e + k_h \times SP^h\right)d^n. \tag{14}$$

SP^e is the investment cost of the wind park per capacity unit.

SP^h is the investment cost of the PtG system per capacity unit.

d^n is the depreciation factor in year n. If the firm follows a straight-line depreciation schedule over the useful lifetime then $d^n = 1/T$; other options can be considered, e.g. accelerated depreciation.

Note that the variable operating cost of the PtG system is included in Eq. (4) via w^h, while that of the wind power plant is assumed to be zero. This is for simplicity; according to IRENA [39], the average O&M cost of onshore wind ranges from 0.006 \$/kWh to 0.02 \$/kWh for most of countries and projects. In Armijo and Philibert [40] it is set at 2 % of capex per year. In Coppitters et al. [15] it ranges between 18 and 36 €/kw/year.

The present value of income taxes is:

$$TX = \propto \sum_{n=1}^{30} TI_n e^{-r(n+1)} \tag{15}$$

α is the corporate tax rate (assumed constant). The authors assume that the corporate tax on year-n income is payed off in year $n + 1$.

In sum, the net present value of the combined system is:

$$NPV = V_0 - TX - \left(SP^e + k_h \times SP^h\right) \tag{16}$$

This NPV is to be maximized by choosing a (optimal) value of k_h.

3. Data analysis

The authors separate the parameter estimates of the stochastic variables on one hand and the parameter information for the valuation model on the other.

Table 3
Parameter estimates of deterministic part of capacity factor, $D^{CF}(t)$.

Parameter	Coefficient	Std. Dev. *	t value	p value
Constant β_1	24.0865	0.313063	76.94	0.0000 ***
YC β_3	4.32189	0.435859	9.916	0.0000 ***
YC β_4	6.06835	0.449503	13.5	0.0000 ***
YC β_7	−1.57587	0.427123	−3.69	0.0002 ***
YC β_{11}	1.0867	0.429792	2.528	0.0115 **
DC β_{19}	−1.71387	0.117623	−14.57	0.0000 ***
DC β_{20}	2.01344	0.119096	16.91	0.0000 ***
DC β_{21}	0.208998	0.053937	3.875	0.0001 ***
DC β_{22}	−0.44134	0.051197	−8.62	0.0000 ***
DC β_{23}	−0.17697	0.032812	−5.393	0.0000 ***
DC β_{24}	0.282881	0.032886	8.602	0.0000 ***
DC β_{25}	0.058774	0.025405	2.314	0.0207 **
DC β_{28}	−0.06573	0.02226	−2.953	0.0031 ***

* HAC standard deviations, with bandwidth 24 (Bartlett Kernel). Source: Authors calculations. Note: Asterisks denote statistical significance at levels: *** 0.1%; ** 1%.

3.1. Risk factors.

3.1.1. Estimation.

Given that the first year in the sample (2016) is a leap year, the first hour of the time series corresponds to $t = 1/366/24$. For 2017, 2018, and 2019 the hourly increments are $1/365/24$. Looking ahead, for getting a forecast, it is necessary to know the time t that corresponds to every hour in the year, the day of the week (for the dummy variables) and the hour of the day (for the index τ). The numerical estimates of β_k^i ($k = 1, 2, …, 28$) are taken to Eqs. (1) - (3), and these in turn to Eq. (2).

Table 2 shows the parameter estimates of the deterministic part of electricity price ($D^E(t)$). The constant is 37.41 €/MWh, and the price grows by 2.871 €/MWh every year. The YC parameters describe the yearly cycle. All of the parameters of the weekly cycle WC are statistically significant. The DC parameters show the hourly behavior within a day.

Table 3 shows the parameter estimates of the deterministic part of capacity factor ($D^{CF}(t)$). The mean CF is 24.0865 %. In this case, there seems to be no time trend. None of the parameters of the weekly cycle WC is significant; CF does not change depending on the day of the week.

Parameters in Tables 2 and 3 are estimated by ordinary least squares (OLS). Standard errors are robust to heteroskedasticity and autocorrelation (HAC) following Newey and West [41]. Now, just to avoid any false sense of stability in our risk factors, Fig. 4 displays the hourly power price and capacity factor as forecasted by the model with the above estimates for a single month, namely January 2016.

$D^{CF}(t)$(red line) displays an hourly cycle with 31 peaks and troughs; any additional yearly cycle is harder to grasp. There is a similar hourly cycle for $D^E(t)$ (blue line) along with a weekly cycle. Note again that the authors account only for those variables which are statistically significant (at the 1 % level).

Regarding the stochastic part, S_t^i, for estimation purposes the time lapse dt is approximated by $\Delta t = 1/(365 \times 24)$. Table 4 shows the parameter estimates of both S_t^E and S_t^{CF}.

3.1.2. Simulation.

Typically there is a relationship between the number of random inputs, simulated paths, and step frequency. For example, Kroniger and
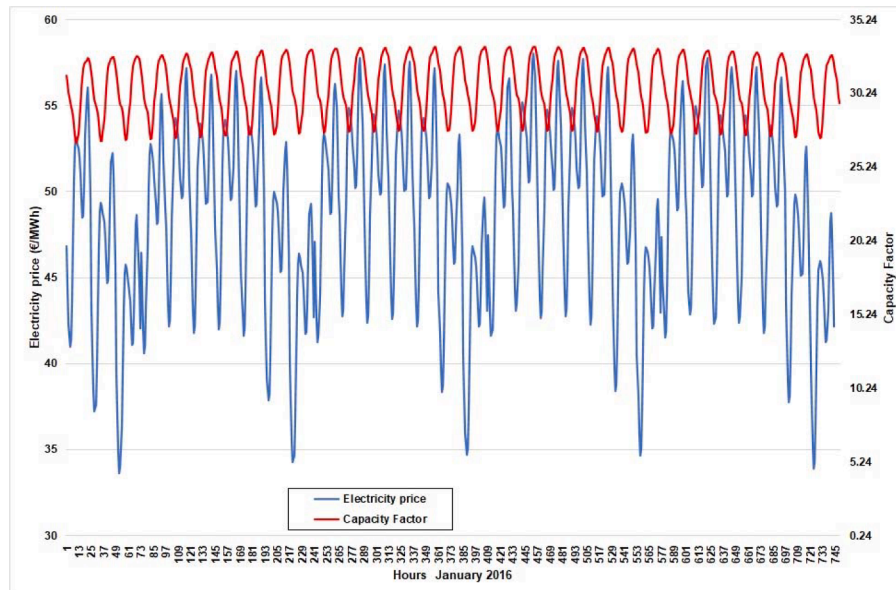

Fig. 4. Forecast deterministic hourly capacity factor and power price for January 2016.

Table 4
Parameter values of stochastic components S_t^i and confidence intervals.

Electricity (S_t^E)		Capacity Factor (S_t^{CF})	
Parameter Value	90 % Interval	Parameter Value	90 % Interval
α^E 1290.842	1082.825–1498.859	α^{CF} 389.896	206.011–573.782
κ^E 133.2616	149.495–117.028	κ^{CF} 58.066	68.551–47.581
μ_j^E −0.66366	−0.793 - −0.535	μ_j^{CF} −0.174	−0.249 - −0.099
σ^E 151.6248	149.165–154.045	σ^{CF} 106.989	103.935–109.958
σ_j^E 4.370776	4.26–4.479	σ_j^{CF} 1.971	1.882–2.057
λ^E 1942.015	1832.972–2051.058	λ^{CF} 2225.522	1906.091–2544.953

Table 5
Simulated correlation coefficient between stochastic parts and confidence intervals.

Correlation coefficient	Lower bound (95 %)	Upper bound (95 %)	Lower bound (90 %)	Upper bound (90 %)
−0.4570	−0.4674	−0.4465	−0.4657	−0.4482

Madlener [19] consider three sources of uncertainty, perform 10,000 simulation runs where an iteration step takes one hour, over a 24 h interval. In Grueger *et al.* [20], a single risk factor is simulated over one year with quarter-hourly time steps (i.e. 35,040 steps). In our case, the authors run 1,600 simulations that stretch over 30 years with hourly time steps (thus, 262,992 steps; there are 8 leap years from 2020 to 2049). Each simulation involves (correlated) time paths for the electricity price and the capacity factor. Farhat and Reichelstein [17] simulate a real-life performance following a different approach: they look at a price series over a particular year and assume that it will repeat itself every year throughout the facility's lifetime.

The stochastic parts, $S^E(t)$ and $S^{CF}(t)$, in actual data have a correlation coefficient of −0.4570. Their simulated correlated samples have a coefficient of −0.4578, which is very close to the observed figure. Table 5 shows the simulated correlation coefficient along with two confidence intervals (Long [42]).

3.1.3. Spot prices, futures prices, and present values.

There are two basic approaches to valuing the present value of a future, uncertain cash flow. One consists in adjusting simultaneously for risk and time through a single discount rate (which must be commensurate with the perceived level of risk). The other one proceeds in two steps. First, the uncertain cash flow undergoes a 'haircut' (in the investor's eyes) by translating its mathematical expectation or average value (a statistical construct) into its so-called 'certainty equivalent' (an economic construct, which depends on the investor's behavior toward risk, usually risk aversion). Thus, the average or expected payoff from a lottery ticket (that pays either $200 or 0 with probabilities 50 %-50 %) is $100, but a particular investor may be indifferent between the lottery ticket (which pays $100 on average) and, say, $94 for certain. Next, since the time dimension still remains as such, these $94 must be discounted back to the present; yet, the rate to be used now is the risk-free interest rate (as opposed to the higher, risk-adjusted rate above). Since

using the risk-free rate amounts to leaving any consideration for risk aside, this practice is in effect consistent with investors that are neutral towards risk.

Electricity is actively traded on futures markets. For instance, today (time 0) there is available a contract for delivery of 1 MWh every hour in 2026 in exchange for a fixed amount of money, the futures price. Futures prices are not the spot prices expected to prevail in the physical or actual world in the future, which are harder to estimate (because of the risk premium embedded in actual prices). Finance textbooks show that the futures price for a given maturity is equal to the spot price expected to apply at that time if market agents are risk neutral. Thus, the futures price provides the expected value of the future spot price in a risk-neutral world; consequently, it can be discounted back to the present at the risk-free interest rate. In the case of the euro zone, this rate is typically the interest rate on the 10-year German government bond.

Further, nowadays trade on electricity is not restricted to just one single futures contract; there are several ones, with different delivery (maturity) dates and corresponding futures prices. Therefore, it is possible to fit a curve to the discrete futures prices observable in the market for a set of maturities (e.g. March, June, September, December in a given year). Unfortunately, however, there are electricity futures contracts for delivery up to five years ahead, while the hybrid system's expected lifetime (valuation horizon) is 30 years.

In view of this, the authors take yearly futures contracts (SPEL Base Futures Year) from 2020 to 2026, and set the 2026 price as fixed for all subsequent years through 2049. At the same time, the authors compute the yearly average of the simulated spot power prices from 2020 to 2049. Drawing on these two series the authors compute the implied yearly discount factors; see Fig. 5. It shows the spot prices anticipated to apply in the future (blue line) and the futures prices adopted in this study (brown line). For these two series to be consistent with each other the former must be multiplied by the discount factors underlying the black line; their product yields the futures prices. Take, for example, the year 2049, when the forecast spot price is about 140 €/MWh and the futures prices has been kept flat at some 42 €/MWh. Setting the latter equal to the value of the former discounted back to 2020 at some rate ρ the authors get:

$$42.25 = 139.66 \times e^{-29.5 \times \rho} \rightarrow e^{-29.5 \times \rho} = \frac{42.25}{139.66} = 0.3025 \rightarrow \rho = 0.0405$$
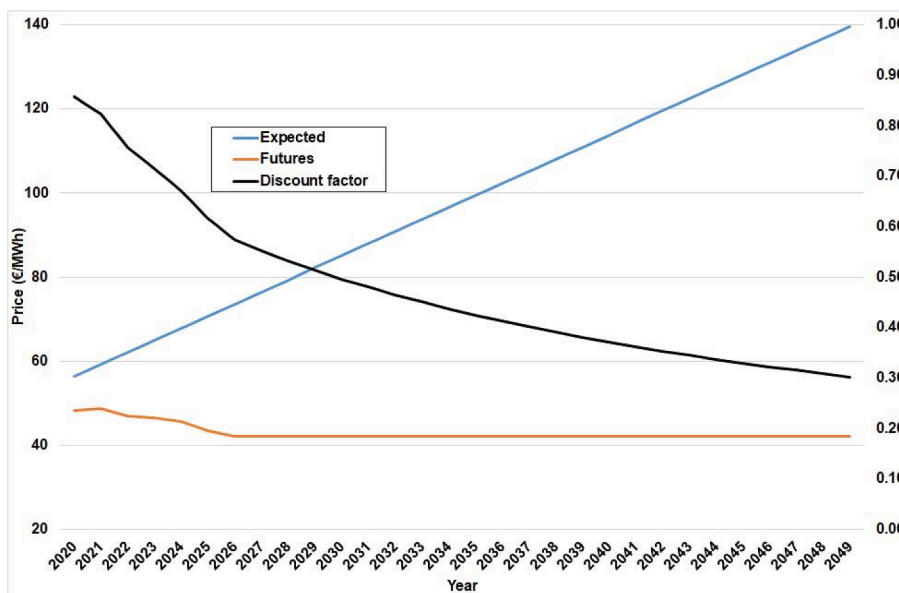
$$\approx 4.05\%.$$

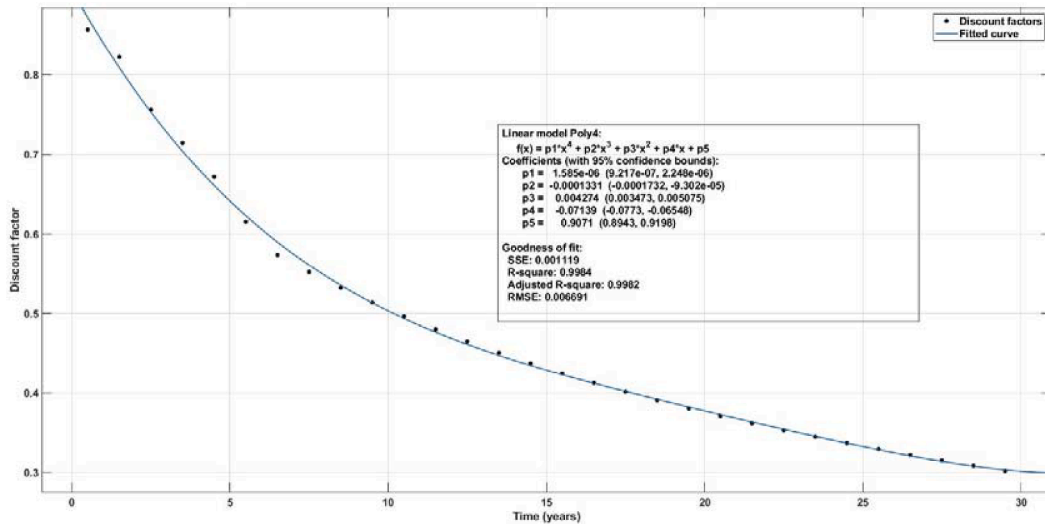**Fig. 5.** Yearly futures prices, simulated spot prices, and implied discount factors.

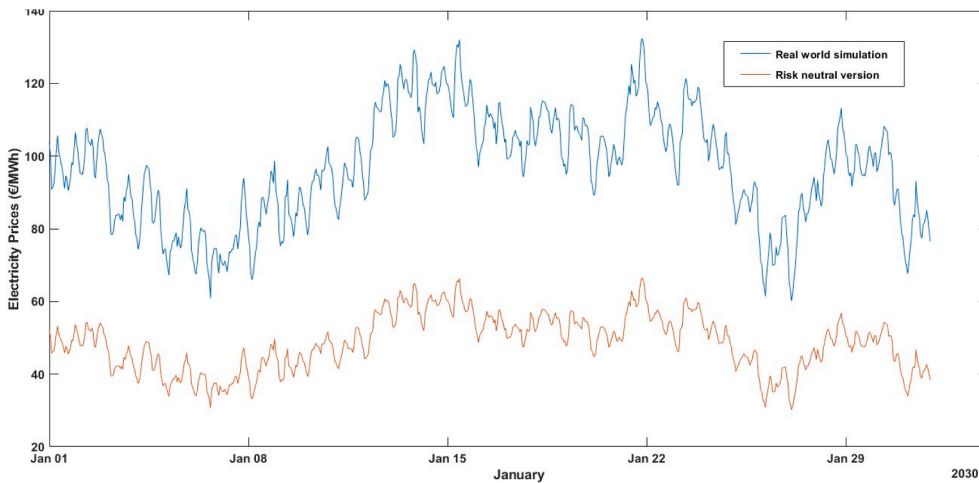**Fig. 6.** Statistical fit to yearly discount factors.

Fig. 7. Simulated power price in the physical world and the risk-neutral world, January 2030.

The average value of ρ over the valuation horizon turns out to be 7.14 %.

Next, as shown in Fig. 6, the authors fit a fourth-degree polynomial to the earlier discount factors. The resulting continuous curve (a declining function of time) allows derive discount factors for any maturity needed, even at an hourly scale. The authors use these factors to compute risk-adjusted values of the simulated electricity price series (to be multiplied later by the electricity output). As usual, the further into the future, the lower the present value. In our view, it can be hard to calculate a discount factor for the CF. Anyway since it is a mean-reverting process (dominated by the deterministic part) the risk should be relatively lower and offset in the long run.

Both Figs. 5 and 6 consider a time horizon that encompasses the expected lifetime of the project (30 years). At this macro scale, everything seems to evolve smoothly over time. However, this smooth appearance can be misleading. Now, Fig. 7 focuses on a much shorter horizon, namely a single month in a particular year: January 2030. At this micro scale, smoothness all but disappears. Randomness is all around emanating from the stochastic part in the spot price of electricity. The blue line depicts the simulated path in the physical, real world. The red line, instead, applies the appropriate discount factor to the former series; it shows the power prices that would be observed in the futures markets (consistent with those spot prices). Again, for these

spot prices to be consistent with the futures prices, discount factors must follow suit.

3.2. Input data for the NPV model.

Table 6 shows the values of the main input variables. The estimate of SP^e is an average of Overnight costs for onshore wind generating technology ($>= 1$ MW) in a sample of countries (Austria, Belgium, Denmark, Finland, France, Italy, Netherlands, Norway, and Sweden), IEA [25]. It is in line with the estimates in Armijo and Philibert [40] for wind turbines Nordex N100-3.3 Class 1 (1,200 $/kW) and Vestas 90–2 Class 2 (1,300 $/kW). It is somewhat lower than 1,367 €/kW used by Glenk and Reichelstein [8]; Duan *et al.* [43] assume 1,319 $/kW. IRENA [44] anticipates the total installed cost to drop further in the coming decades. It also forecasts that ongoing advancements in wind technology and project siting will further improve capacity factors.

The values of SP^h, η, T, α, γ, d^n, w^e, w^h, F^e, and F^h are the same as in Glenk and Reichelstein [8]. Nonetheless, there are a variety in the related literature. For example, the expected lifetime of the wind farm is 25 years in Duan *et al.* [43]. That of the PtG plant in Schultes and Madlener [7] is 23 years, and 16 years in Way *et al.* [10]. The lifetime of the hybrid system in Aguado *et al.* [45] is 20 years, instead of 30 years for both facilities as here. The PtG plant's lifetime is related to the

Table 6
Main parameter values.

Symbol	Variable	Value	Reference
SP^e	Wind power technology's cost	1,200 €/kW	IEA (2020)
SP^h	Power to Gas (PtG) system price	2,287 €/kW	Glenk-Reichelstein [7]
η	Conversion rate	0.019 Kg/kWh	Glenk-Reichelstein [7]
CF_t	Wind capacity factor	Stochastic	
φ	Unused share	0.0774	Appendix A
p_t^e	Electricity price	Stochastic	
r	Discount rate (WACC, real)*	Time varying	
r_f	Risk-free rate	0	European Central Bank
T	Useful lifetime	30 years	Glenk-Reichelstein [7]
α	Income tax rate	35 %	Glenk-Reichelstein [7]
γ	Degradation rate	0.0080	Glenk-Reichelstein [7]
d^n	Depreciation factor	1/16	Glenk-Reichelstein [7]
w^e	Wind energy variable operating cost	0.00 €/Kwh	Glenk-Reichelstein [7]
w^h	PtG variable operating cost	0.10 €/Kg	Glenk-Reichelstein [7]
FC^e	Wind energy fixed operating costs	38.00 €/kW	Glenk-Reichelstein [7]
FC^h	PtG fixed operating costs	45.00 €/kW	Glenk-Reichelstein [7]

* The authors have discounted our (simulated) future electricity prices with different discount factors (see Fig. 6 in Section 3.1.3) so as to make them consistent with (observed) electricity prices in futures markets. The latter must be discounted at the risk-free rate, in our case the 10-year German Treasury bond, which is essentially zero right now. Concerning the future hydrogen price the authors have no particular clue; whatever it happens to be, the authors assume that the future price discounted back to the present equals its current price, p_t^h.

electrolyzer stack lifetime (i.e. operating hours) and the utilization rate. Thus, Way *et al.* [10] look at PEM technology and assume a lifetime of 70,000 h. This translates into 7.99 years if the electrolyzer is operated at an average utilization rate of 100 %; instead, at 50 % utilization rate the earlier lifetime translates into around 16 years. In some instances, the same variables are stated in different units. Thus, Schultes and Madlener [7] express the operation expenditures of the PtG plant as a percentage of the specific investment costs per year. Similarly, here CF^e is 38.00 €/kW but 26.22 $/kW in Duan *et al.* [43].

Regarding η, typical PEM electrolyzers reach conversion efficiencies in the range 65 % to 83 % (based on hydrogen's higher heating value); Gahleitner [5]. Way *et al.* [10] assume it is 70 %, the same as in Armijo and Philibert [40]. Touili *et al.* [11] consider an electrolyzer that consumes 53 kWh in order to produce 1 kg of hydrogen which is equivalent to 75 % efficiency; this means a conversion factor of 1/53 = 0.018868. Mohsin *et al.* [34] claim 53.4 kWh, or a factor 1/53.4 = 0.01873. Our rate here, 0.019, implies that 52.63 kWh are required to produce 1 kg H_2. In Eypasch *et al.* [21] electrolysis efficiency ranges from 60 % to 84 %; they eventually adopt a conservative value of 65 %, the same as Grueger *et al.* [20]. In Mohsin *et al.* [34] it is between 56 % and 75 %. Green *et al.* [46] consider both 63 % and 74 % in their analysis.

Concerning CF_t, Duan *et al.* [43] use for Spain an annual mean wind capacity factor of 0.32; IRENA [39] reports an average of 27 % in 2010 and 38 % in 2020. According to Coppitters *et al.* [15] it is 23.1 % for Belgian onshore wind farms; they consider a range between 20 % and 26 %. These numbers are well below those reported by Armijo and Philibert [40] for the best sites in Argentine and Chile, where CF reaches up to 52.7 %. The unused share (φ) in Kroniger and Madlener [19] goes from 0.012 to 0.26 with an average of 0.139 for Germany over 2004–2011. For Scottish onshore farms, the volume-weighted average curtailment

Table 7
Hybrid system's NPV (in €) for different pairs of hydrogen price and PtG capacity (0.05 MW increments).

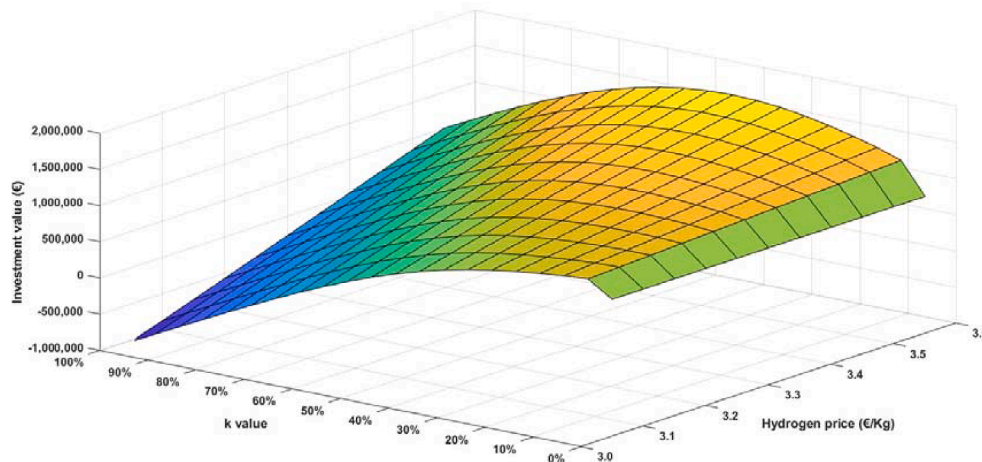|		Hydrogen price (p_h)										
		3.0	3.1	3.2	3.3	3.4	3.5	3.6	3.7	3.8	3.9	4.0
PtG capacity (k_h)	0	894,165	894,165	894,165	894,165	894,165	894,165	894,165	894,165	894,165	894,165	894,165
	0.05	**1,109,517**	**1,130,759**	1,152,191	1,173,759	1,195,422	1,217,150	1,238,926	1,260,735	1,282,568	1,304,419	1,326,282
	0.1	1,087,554	1,121,859	**1,156,481**	1,191,310	1,226,274	1,261,339	1,296,475	1,331,658	1,366,878	1,402,127	1,437,396
	0.15	1,052,722	1,099,742	1,147,021	**1,194,467**	1,242,028	1,289,649	1,337,319	1,385,030	1,432,767	1,480,534	1,528,321
	0.2	1,011,811	1,071,590	1,131,387	1,191,119	**1,250,768**	1,310,370	1,369,930	1,429,472	1,489,012	1,548,559	1,608,119
	0.25	962,621	1,035,262	1,107,481	1,179,189	1,250,460	**1,321,392**	1,392,104	1,462,674	1,533,159	1,603,607	1,674,045
	0.3	903,032	988,412	1,072,953	1,156,422	1,238,869	1,320,528	**1,401,620**	1,482,339	1,562,829	1,643,181	1,723,467
	0.35	831,238	928,955	1,025,468	1,120,434	1,213,755	1,305,616	1,396,393	**1,486,412**	1,575,927	1,665,143	1,754,176
	0.4	745,885	855,140	963,089	1,069,077	1,172,910	1,274,650	1,374,567	1,473,163	1,570,839	**1,667,898**	1,764,592
	0.45	646,451	765,912	884,344	1,000,755	1,114,615	1,225,843	1,334,629	1,441,312	1,546,463	1,650,556	1,753,921
	0.5	533,196	661,221	788,705	914,532	1,037,800	1,158,092	1,275,394	1,389,995	1,502,270	1,612,808	1,722,159
	0.55	407,280	541,923	676,804	810,571	942,236	1,070,992	1,196,481	1,318,732	1,438,083	1,554,934	1,669,840
	0.6	270,378	409,788	550,161	690,246	828,843	965,065	1,098,182	1,227,857	1,354,140	1,477,360	1,597,929
	0.65	124,341	267,036	411,178	555,768	699,732	842,003	981,761	1,118,341	1,251,398	1,380,976	1,507,362
	0.7	-28989	115,844	262,463	410,002	557,640	704,461	849,511	991,999	1,131,342	1,267,167	1,399,474
	0.75	-187944	-41744	106,394	255,779	405,724	555,538	704,438	851,582	996,198	1,137,764	1,275,891
	0.8	-351007	-204002	-54951	95,499	246,812	398,443	549,794	700,214	848,930	995,232	1,138,607
	0.85	-516971	-369485	-219928	-68886	83,172	235,817	388,619	541,057	692,582	842,494	990,145
	0.9	-684879	-537123	-387280	-235928	-83489	69,685	223,250	376,864	530,070	682,411	833,251
	0.95	-854032	-706125	-556131	-404615	-251989	-98570	55,383	209,585	363,765	517,523	670,464
	1	-1023943	-875958	-725883	-574286	-421569	-268035	-113921	40,575	195,223	349,800	503,964

Fig. 8. Hybrid system's NPV (in €) as a function of hydrogen price and PtG capacity.

during 2012–2016 was 10.61 %; instead, Germany's average over the same period was 2.98 % (Joos and Staffell [35]).

As for the WACC, it must be a real rate (rather than nominal), because LCOE or LCOH are measured in constant monetary units; Reichelstein and Sahoo [23]. It must also be after tax (instead of pre-tax), since the authors adopt the viewpoint of potential investors. Aguado *et al.* [45] adopt 3 % for Spain. Glenk and Reichelstein [8] use 4 % for Germany and 6 % for Texas; Shaner *et al.* [9] use 12 % for solar in the U.S.; Touili *et al.* [11] assume 6 % for solar in Morocco. In Armijo and Philibert [40] the WACC ranges between 7 % and 10 % for a hybrid solar/wind system in Argentine and Chile. Stöckl *et al.* [4] use an interest rate 4 % for Germany in 2030. Coppitters *et al.* [15] use a range between 5 and 7 % for Belgium. Kroniger and Madlener [19] assume the IRR to be 4 % for Germany. Talebian *et al.* [14], instead, opt for 10 % in British Columbia. Grueger *et al.* [20] adopt an interest rate of 5 % for Germany in 2013. Eypasch *et al.* [21] set the rate of interest and the depreciation period at 12 % p.a. and 15 years for infrastructural investment cost calculations for a BMW Group production site located in Germany. The depreciation of capital investment on all the equipment is calculated by the annuity method to distribute the capital expenditure over the life-time of the equipment. For stack exchange, an expense of 60 % of capital cost after 8 years is included; stack exchange is required only once during the considered depreciation period of the complete system of 15 years. Glenk and Reichelstein [8] adopt a linear depreciation schedule over 16 years for Germany (i.e. 6.25 % per year). Van Benthem [12] for Japan: 7 % risk-adjusted discount rate (WACC); 4 % risk-free interest rate. Schultes and Madlener [7]: risk-free interest rate of 12 %. Duan *et al.* [43]: discount rate of 7 % in determining the cost of capital recovery for the technologies considered; the same as in Guerra *et al.* [13]. Steffen [47] overviews the spectrum of estimation methods and numerical estimates for the private cost of capital for VRE projects in 46 countries in 2009–2017. For onshore wind, the 2017 average WACC for OECD countries is 7.3 %, and 10.4 % for non-OECD. IRENA [39] shows an average WACC that declines from 7.5 % in 2010 to 5 % in 2020 for OECD countries and China (the figures are 10 % and 7.5 %, respectively, for the rest of the world).

4. Results.

4.1. Combined project NPV.

4.1.1. Our estimates.

As Glenk and Reichelstein [8] point out, each assumed hydrogen price triggers a unique maximizing capacity choice, k_h^*. In this regard, the authors aim at deriving a surface that displays the NPV attached to pairs of hydrogen prices and PtG capacities under the assumption that

both the power market price and the wind capacity factor evolve sto-chastically over time. Optimal conversion capacities are those which maximize NPV for each hydrogen price. The authors run 1,600 simu-lations with hourly time steps that stretch over 30 years. Each simulation involves (correlated) time paths for p_t^e and CF_t. Simulation results allow compute not only average or expected values (e.g. the NPV). They allow to derive the frequency or probability distribution ('risk profile') as well, which conveys a deeper understanding of the investment project and enables investors to compute other metrics typically used in project evaluation (e.g. the value at risk, VaR).

In the following numerical results the wind farm's capacity is set at $k_e = 1$ MW. The authors adopt a wind capacity factor of 38 % (which corresponds to France; IEA [25]). The resulting project value is NPV = 894,165 € per MW of wind capacity. Thus, the wind facility is profitable on its own ($k_h = 0$). The CF is the subject of a sensitivity analysis later on; changes in the average level reflect the overall (age-based) efficiency of the wind park.

Table 7 shows the hybrid system's NPV (in €) for different pairs of PtG capacity (first column) and hydrogen price (first row). The yellow shade identifies the highest NPV (and k_h^*) for a given p_h. At the high end, when $p_h = 4$ €/kg the authors get $k_h^* = 0.40$ MW (i.e. 40 % of the normalized wind capacity $k_e = 1$ MW). Instead, for a low $p_h = 3.2$ €/kg the optimal capacity is small, $k_h^* = 0.10$ MW.

Fig. 8 displays the NPV as a function of both p_h and k_h. Above $p_h = 3$ €/kg the authors observe that moving from a wind facility alone ($k_h = 0$) to a hybrid system increases the project's NPV (green edge furthest to the right). Henceforth, with $p_h = 3.0$ €/kg and 3.1 €/kg the NPV de-creases monotonically, turning to negative for k_h above 0.7 MW. Nonetheless, starting from $p_h = 3.2$ €/kg and upward there is some scope for higher NPVs accompanied by bigger PtG capacities but up to a point (yellow area at the top); in the hydrogen price range considered here, k_h^* never surpasses 0.31 MW. Above this threshold the NPV declines. On the other hand, the NPV remains positive even with $k_h = 1.0$ MW pro-vided the hydrogen price is $p_h = 3.7$ €/kg at least.

4.1.2. Comparison with the related literature.

How do these numbers compare with previous results in the litera-ture? Glenk and Reichelstein [8] apply their model to wind parks in different contexts over a time horizon of 1 year (i.e. $365 \times 24 = 8,760$ h). They find hydrogen break-even prices of 3.23 €/kg H_2 in Germany and 3.53 $/kg H_2 in Texas. In both cases the power price used is time invariant (0.0318 €/kWh in Germany and 0.0255 $/kWh in Texas). Armijo and Philibert [40] get a lower estimate of about 2 $/kg for hybrid wind/solar plants in some sites of Argentine and Chile.

Hosseini *et al.* [48] reports the cost of hydrogen from various pro-duction processes. Natural gas reforming entails a cost of 1.03 $/kg;
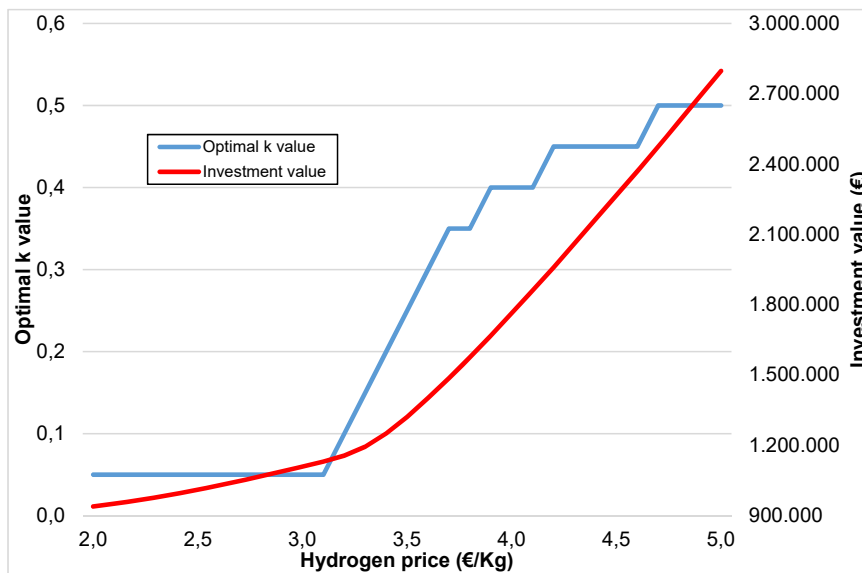
Fig. 9. Impact of hydrogen price on optimal PtG capacity and project NPV.
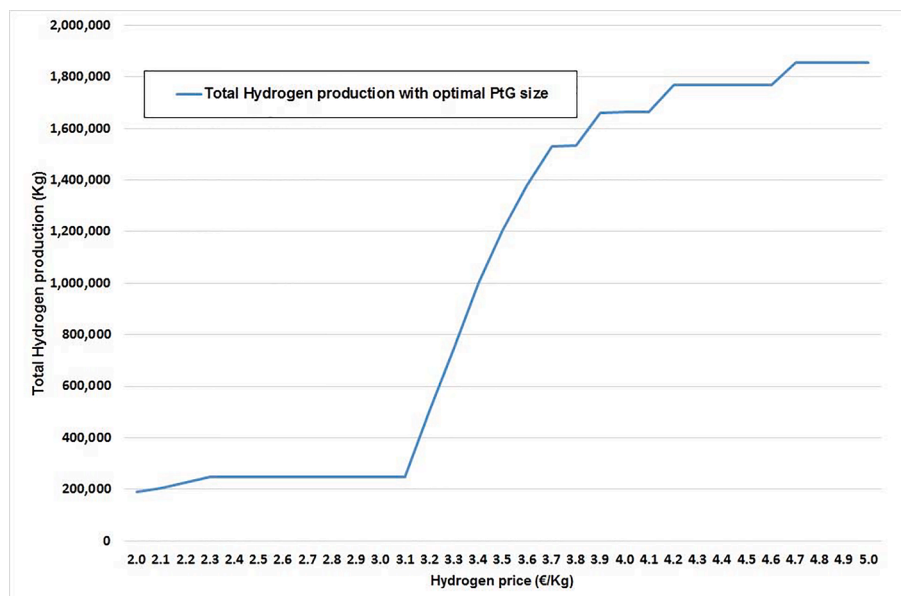

Fig. 10. Hydrogen production with efficiently sized PtG capacity.

wind electrolysis, instead, incurs a cost of 6.64 $/kg. Note that the efficiency of the former process falls in the range [70–85 %], while in the latter it is [50–70 %]. Nikolaidis and Pollikkas [3] provide a hydrogen cost from wind electrolysis in the range 5.89–6.03 $/kg, and 2.08 $/kg from natural gas reforming (both costs in 2005-dollars). More recently, Jaunatre [6] estimates the cost of hydrogen from fossil fuels between 1 and 1,5 €/kg, while that of renewable hydrogen ranges between 3 and 6 €/kg depending on the VRE source. Thus, it is about 5–6 €/kg from wind power, and 3–5 €/kg from solar PV. Coppitters *et al.* [15] provide a similar comparison. Coal gasification sets the lower bound with a range 1.11–1.35 €/kg. For wind hydrogen the cost ranges between 4.40 and 5.00 €/kg. These costs can be pushed down by increasing the production scale and decreasing the purity requirement, but not enough for renewable hydrogen to be cost-competitive with fossil-based hydrogen. To reach parity requires support via public policy.

4.2. Optimal conversion capacity and hydrogen production.

4.2.1. Our estimates.

Fig. 9 shows how the optimal PtG capacity increases as the hydrogen price gets higher. k_h essentially takes off for hydrogen above 3.1 €/kg. From that price level on, it follows a step-by-step path. The same applies to the hybrid project's NPV. There is clearly a first part of mild growth, followed by a second one of strong growth from 3.2 €/kg onwards.

As can be expected, the amount of hydrogen produced goes hand in hand with the deployment of the PtG capacity. See Fig. 10. The profile resembles pretty much those in Fig. 8.

4.2.2. Comparison with the related literature.

Glenk and Reichelstein [8] find a hydrogen break-even price of 3.23 €/kg H_2 in Germany, with a corresponding optimal PtG capacity smaller than ours (0.10 kW), namely $k*_h = 0.01$ kW.

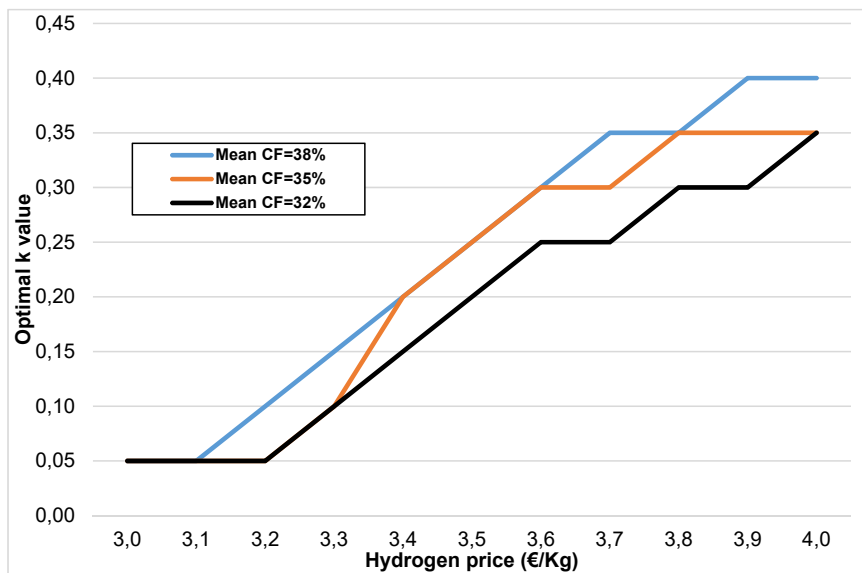Note anyway that their calculations proceed in increments of 0.01

Fig. 11. Wind CF and the relationship between hydrogen price and PtG capacity.
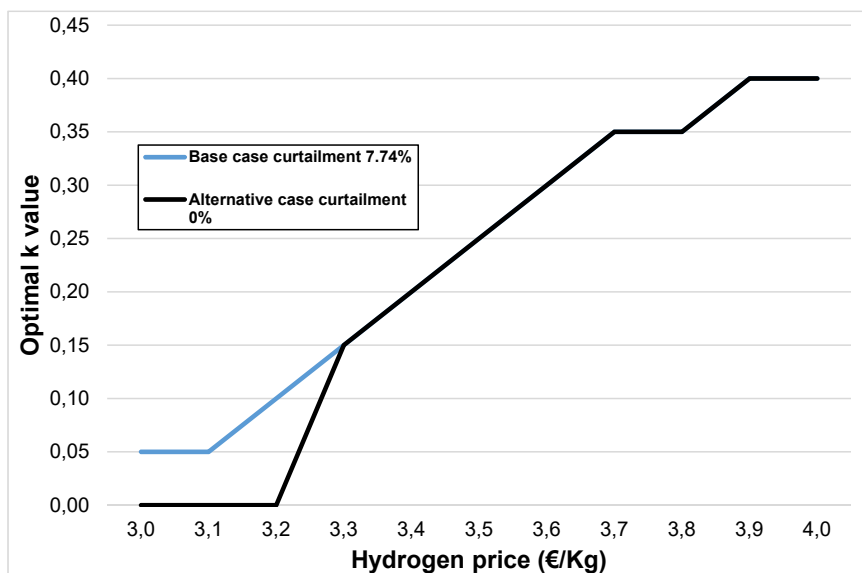

Fig. 12. Wind curtailment and the relationship between hydrogen price and PtG capacity.

kW, while our increments are 0.05 kW. The authors consider 0.01 kW increments in Table A2 in the APPENDIX C for comparison purposes. According to our results, for $p_h = 3.2$ €/kg the optimal capacity is $k^*_h = 0.07$ kW, somewhat smaller than in the previous paragraph. In a sense, the authors reach the same qualitative result as Glenk and Reichelstein [8]: production of green hydrogen can be cost competitive with small- and medium-scale fossil hydrogen production (above 3 €/kg H_2), but not with large-scale supply (below 2.5 €/kg H_2).

5. Sensitivity analyses.

Now, the authors undertake three sensitivity analyses. The first two address the consequences of changes (or forecast errors) in two key project variables, both of them related to the wind energy. The third one involves a different valuation approach. Specifically, instead of resorting to time-varying discount rates in the risk-neutral world, the authors adopt a constant, risk-adjusted discount rate applying in the physical world, which is in line with standard practice in the related literature.

5.1. Average wind capacity factor.

First, the authors analyze the impact of hydrogen price on k_h under different values of CF. Remember that at any time the authors keep the stochastics of the original Spanish time series but the average value is not the original one (24.09 %) but a higher one to better capture young wind parks instead of the older ones. Thus, along with the average underlying our previous estimates (38 %) the authors also consider two other, lower ones. Intuition suggests that recent wind facilities should be better suited for exploiting PtG synergies via higher conversion capacities.

As shown in Fig. 11, the lowest CF is associated with the lowest curve (as seen from the horizontal axis). This means that, for any hydrogen price considered, the optimal conversion capacity is lowest when CF is lowest (namely 32 %). Then, as the latter rises to 35 %, for p_h above 3.3 €/kg the optimal k_h increases and remains above the earlier curve over the price range considered. When CF is highest (38 %), for any p_h above 3.1 €/kg the optimal capacity is even higher than before and remains

Table 8

Hybrid system's NPV (in €) for different pairs of hydrogen price and PtG capacity: flat discount rate $r = 5.1$ %.

PtG capacity (k_h)	Hydrogen price (p_h)										
	3.0	3.1	3.2	3.3	3.4	3.5	3.6	3.7	3.8	3.9	4.0
0	1,011,085	1,011,085	1,011,085	1,011,085	1,011,085	1,011,085	1,011,085	1,011,085	1,011,085	1,011,085	1,011,085
0.05	**1,218,430**	**1,237,944**	**1,257,870**	1,278,152	1,298,738	1,319,580	1,340,636	1,361,868	1,383,242	1,404,731	1,426,311
0.1	1,191,595	1,222,387	1,253,968	**1,286,234**	1,319,077	1,352,412	1,386,155	1,420,238	1,454,594	1,489,169	1,523,919
0.15	1,152,788	1,194,305	1,236,921	1,280,485	**1,324,862**	1,369,928	1,415,564	1,461,674	1,508,172	1,554,984	1,602,040
0.2	1,109,111	1,161,149	1,214,491	1,268,952	1,324,364	1,380,579	1,437,485	1,494,965	1,552,919	1,611,255	1,669,900
0.25	1,058,579	1,121,022	1,184,830	1,249,783	1,315,705	**1,382,451**	1,449,911	1,517,976	1,586,557	1,655,564	1,724,916
0.3	998,704	1,071,617	1,145,782	1,220,926	1,296,874	1,373,523	**1,450,778**	1,528,581	1,606,866	1,685,566	1,764,617
0.35	927,148	1,010,435	1,094,912	1,180,117	1,265,766	1,351,786	1,438,138	**1,524,832**	**1,611,869**	**1,699,234**	1,786,900
0.4	842,033	935,361	1,029,915	1,125,030	1,220,248	1,315,294	1,410,215	1,505,089	1,600,001	1,695,036	**1,790,235**
0.45	742,614	845,126	949,180	1,053,801	1,158,304	1,262,272	1,365,494	1,468,058	1,570,191	1,672,062	1,773,819
0.5	628,923	739,498	852,031	965,432	1,078,762	1,191,283	1,302,686	1,412,820	1,521,797	1,629,957	1,737,572
0.55	502,006	619,160	738,854	859,935	981,257	1,101,879	1,221,118	1,338,692	1,454,548	1,568,834	1,681,902
0.6	363,627	485,770	611,111	738,419	866,562	994,411	1,121,025	1,245,795	1,368,428	1,488,976	1,607,594
0.65	216,000	341,642	471,014	603,024	736,543	870,364	1,003,479	1,134,970	1,264,230	1,391,022	1,515,395
0.7	61,275	189,210	321,238	456,440	593,804	732,230	870,577	1,007,891	1,143,309	1,276,228	1,406,438
0.75	−98735	30,628	164,317	301,524	441,356	582,923	725,179	867,091	1,007,715	1,146,292	1,282,224
0.8	−262573	−132331	2344	140,718	282,052	425,529	570,340	715,569	860,265	1,003,516	1,144,633
0.85	−429031	−298306	−163070	−24021	118,124	262,720	409,044	556,358	703,882	850,726	996,071
0.9	−597233	−466234	−330703	−191316	−48715	96,454	243,615	392,151	541,387	690,670	839,193
0.95	−766548	−635402	−499712	−360152	−217349	−71879	75,701	224,872	375,114	525,833	676,461
1	−936544	−805320	−669551	−529905	−387001	−241406	−93629	55,862	206,600	358,156	510,015

Table A1

shows the full set of results. Standard deviations are robust to heteroscedasticity (HC1 variant).

Table A1.	Coefficient	Stad. Dev	z	p value	
Wind share	0.154797	0.0232622	6.654	<0.0001	***
Mean of dep. vble.	3.247859			S.D. of dep. vble.	3.231059
Sum of squared residuals	613.5796			S.D. of regression	3.096317
R-square	0.546773			Adjusted R-square	0.546773
F(1, 64)	44.28184			p value (F)	7.49e-09
Log-likelihood	−165.1910			Akaike's criterion	332.3820
Schwarz's criterion	334.5564			Hannan-Quinn criterion	333.2399

steadily so. In sum, the higher the average wind CF, the higher the optimal PtG capacity for a given hydrogen price.

Alternatively, looking from the vertical axis, the right-most curve (CF = 32 %) suggests that the optimal deployment of PtG capacity requires the highest hydrogen prices. When the average wind CF grows to 35 % deploying a given conversion capacity is less demanding in terms of p_h. The positive k_h takes off at the same $p_h = 3.2$ €/kg as before (there is actually a positive minimum of k_h because of curtailment), but now it increases more forcefully and evolves above the former curve. An additional improvement in average CF to 38 % brings about a similar impact: k_h starts at a slightly lower p_h, then the new curve overlaps with the 35 % curve, just to evolve above it beyond 3.6 €/kg. Summing up, the higher the average wind CF, the lower p_h needs to be for a given optimal conversion capacity.

5.2. Wind power curtailment rate.

Next, the authors address the impact of wind power curtailment on the relationship between p_h and k_h; see Fig. 12. Up to now, the authors have adopted a rate of 7.74 %; here the authors also consider a 0 rate. The difference between the two patterns turns up at the bottom hydrogen prices, i.e. when the room for the conversion technology cannot be taken for granted. In this regard, a positive rate of curtailment 'helps' the early deployment of PtG capacity (in the end, it is a way to avoid wasting valuable power away). In other words, if the full technical yield from the wind park can be taken to the power market, doing so seems to be the optimal decision under the prevailing circumstances. Nonetheless, for higher hydrogen prices, deploying PtG capacity makes economic sense whether curtailment is zero or 7.74 %; the two patterns overlap.

5.3. A constant risk-adjusted discount rate.

Last, following standard practice, the authors consider a flat discount rate over the whole valuation horizon (as opposed to our time-varying discount factors and underlying rates). In the related literature, the after-tax WACC takes on a number of different values; see Section 4. Here the authors adopt a rate $r = 5.1$ %, the one for onshore wind France (Steffen [47]); note that in our calculations above the average rate over the 30-year period is 7.14 %. In principle, a lower rate will increase the value of the hybrid project (indeed, of any long-lived technology, the more so for capital-intensive ones). Hence, it would seem that, by making the PtG capacity more attractive, this should pave the way for its (relatively) earlier deployment. Nonetheless, a lower rate also changes the time distribution of that value: most of it accrues (relatively) less in the first years and more in the far ahead years. This in turn can have an impact on firm's incentives when deciding which timeline to invest over.

The pattern of PtG deployment turns out to be different in Tables 7 and 8. Thus, starting from the lowest hydrogen prices, for both $p_h = 3.0$ and 3.1 €/kg the optimal conversion capacity is the same, namely 0.05

Table A2
Hybrid system's NPV (in €) for different pairs of hydrogen price and PtG capacity (0.01 kW increments).

|	$p_h = 3.0$	3.1	3.2	3.3	3.4	3.5
$k_h = 0$	894,165	894,165	894,165	894,165	894,165	
0.01	966,754	972,065	977,418	982,802	988,208	
0.02	1,028,226	1,038,415	1,048,685	1,059,011	1,069,377	
0.03	1,073,097	1,087,577	1,102,177	1,116,859	1,131,601	
0.04	1,099,205	1,117,334	1,135,619	1,154,015	1,172,489	
0.05	1,109,517	1,130,759	1,152,191	1,173,759	1,195,422	
0.06	**1,109,976**	**1,133,996**	1,158,238	1,182,637	1,207,144	
0.07	1,105,866	1,132,511	**1,159,406**	1,186,473	1,213,662	
0.08	1,100,157	1,129,371	1,158,860	1,188,534	1,218,340	
0.09	1,093,959	1,125,723	1,157,785	1,190,044	1,222,438	
0.10	1,087,554	1,121,859	1,156,481	1,191,310	1,226,274	
0.11	1,080,981	1,117,822	1,154,992	1,192,376	1,229,896	
0.12	1,074,226	1,113,608	1,153,314	1,193,238	1,233,295	
0.13	1,067,275	1,109,201	1,151,435	1,193,882	1,236,461	
0.14	1,060,110	1,104,585	1,149,343	1,194,297	1,239,377	
0.15	1,052,722	1,099,742	1,147,021	**1,194,467**	1,242,028	
0.16	1,045,094	1,094,657	1,144,454	1,194,379	1,244,397	
0.17	1,037,206	1,089,316	1,141,623	1,194,016	1,246,473	
0.18	1,029,042	1,083,702	1,138,513	1,193,363	1,248,237	
0.19	1,020,583	1,077,800	1,135,107	1,192,403	1,249,675	
0.20	1,011,811	1,071,590	1,131,387	1,191,119	1,250,768	
0.21					1,251,500	1,313,419
0.22					**1,251,853**	1,316,065
0.23					1,251,810	1,318,286
0.24					1,251,352	1,320,068
0.25					1,250,460	1,321,392
0.26					1,249,118	1,322,242
$k_h = 0.27$					1,247,306	**1,322,597**
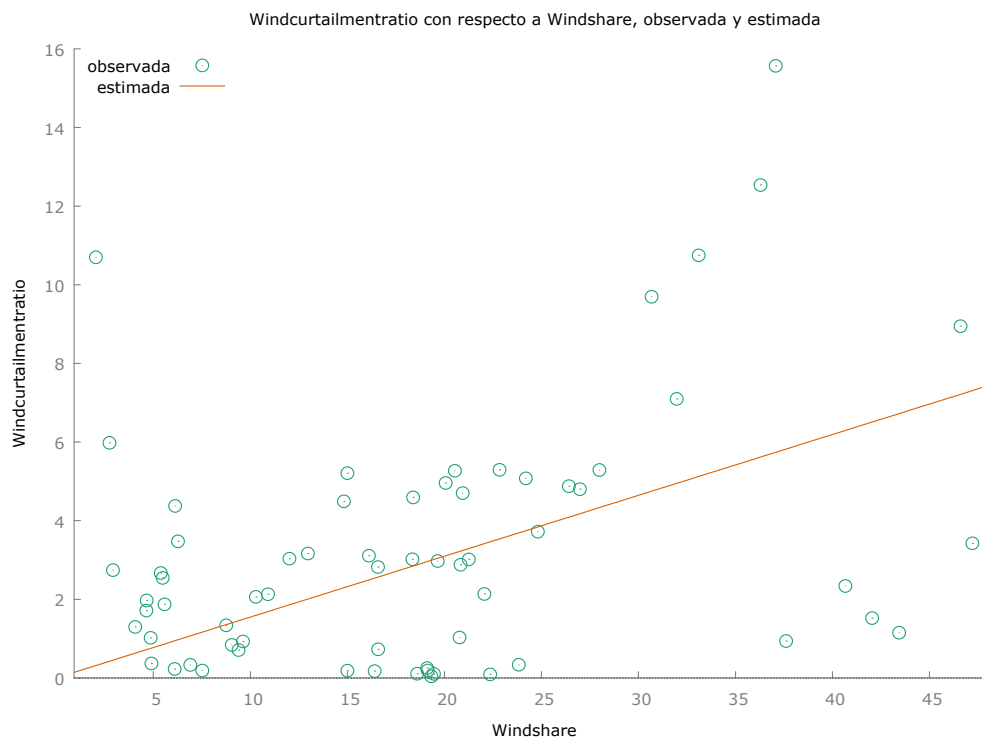
Fig. A1. Share of wind energy and wind curtailmente ratio in several European countries.

kW; this happens in both Tables. Now, for $p_h = 3.2$ €/kg the optimal k_h increases from 0.05 kW to 0.10 in Table 7, but remains stuck at 0.05 kW in Table 8. More in general, optimal conversion capacities tend to be bigger (for the same hydrogen prices) in Table 7 than in Table 8. In other words, the downward yellow stairs are further to the left in Table 7 than in Table 8. This suggests that a fixed discount rate $r = 5.1$ % is hampering the deployment of PtG facilities (relative to the time-varying discount rates in the base case).

On the other hand, the project value is higher with the constant, relatively lower rate $r = 5.1$ %. For one, the wind park alone goes from a NPV = 894,165 € in Table 7 to 1,011,085 € now, an increase of 13 %. In the bottom-right corner ($k_h = 1.0$ kW, $p_h = 4.0$ €/kg) the hybrid project's NPV jumps from 503,964 € in Table 7 to 510,015 € in Table 8, a 1.2 % rise.
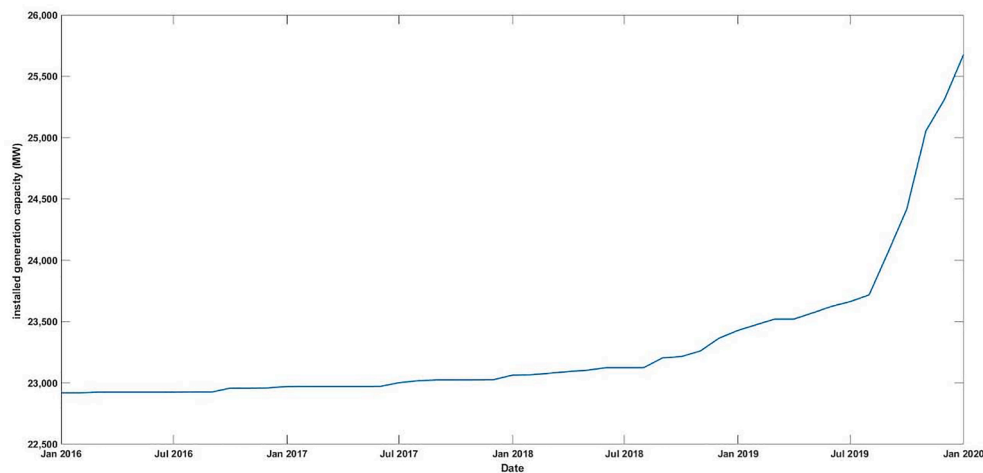
Fig B1. Installed generation capacity of onshore wind farms in Spain, 2016–2019.

6. Concluding remarks

Hydrogen is key to the transition toward a low-carbon economy. Electrolytic production of green hydrogen in particular has sizeable potential to reduce GHG emissions. However, when evaluated from the viewpoint of a potential corporate investor, prospects fall short of this potential. Thus, a number of papers that focus on decarbonizing power generation come to this conclusion.

Nonetheless, to assess properly these results it is necessary to pay attention to the details. For instance, considering hourly time steps over a single year is not unusual. Sometimes commodity prices are assumed to be fixed over time, or the wind capacity factor runs at its average value. Other papers acknowledge the uncertain character of these variables but adopt stochastic processes that are unable to account for the complex dynamics underlying them. Regarding the empirical applications, typically optimization and/or simulation play a limited role.

This study introduces a stochastic model for both the electricity spot price and the wind capacity factor. These state variables show distinctive seasonalities, e.g. yearly, weekly, and daily cycles. Further, these cycles overlap with mean reversion and jumps. The stochastic processes here thus account for both continuous and discrete shocks. We separate the whole dynamics into a deterministic part and a stochastic part. The model is then estimated for a wind park in Spain. Later on, the numerical estimates are framed within a valuation model that encompasses the whole expected lifetime of the facility (30 years) on an hourly basis; this allows compute the facility's NPV. Note that the manager of the wind park must decide at every hour whether to sell the electricity in the spot market or transforming it into hydrogen. As usual, if the manager is to maximize the value of the facility then she must manage it optimally every hour. This paper performs 10,000 simulation runs; each of them involves the former hourly optimization over a 30-year horizon.

According to our results, green hydrogen production starts becoming economically viable above 3 €/kg. Right now, large-scale facilities can produce fossil-based hydrogen at a cost in the range 1.5–2.5 €/kg. Consequently, green hydrogen seems unable to compete; it can be cost competitive with small- and medium-scale hydrogen supply at best.

Regarding the sensitivity analyses, intuition suggests that, for a given hydrogen price, as the average wind capacity factor increases, the optimal PtG capacity should increase, and conversely. Thus, for a given $p_h = 3.2$ €/kg, the optimal conversion capacity is 0.10 kW when the average CF is 38 %, but it drops to 0.05 kW if the latter falls to 35 %. Similarly, it seems that a significant rate of curtailment should contribute to deploying PtG capacity. This is indeed the case: for $p_h = 3.2$ €/kg, with zero curtailment the optimal conversion capacity is 0 kW, but if curtailment grows to 7.74 % the latter rises to 0.10 kW. As for the discount rate, this paper finds that, for $p_h = 3.2$ €/kg, a time-varying rate

of 7.14 % on average is associated again with an optimal conversion capacity of 0.10 kW, but a flat rate of 5.1 % leads to a lower capacity, namely 0.05 kW. This may perhaps come as a surprise. In principle, a lower discount rate should raise the value of a long-lived PtG facility thus easing its (relatively) earlier adoption. Yet there is a subtle impact: most of the increase in value accrues (relatively) more in the distant future, and not so much in the near future. Firms can well have this in mind when deciding the optimal time to invest.

These results, as usual, are subject to some qualifications. For instance, in a number of day-ahead markets there are penalties for prediction errors leading to imbalances in the real-time operation of the system. This is a particular concern in the case of wind energy; Zheng *et al.* [31]. Nonetheless, this is overlooked here. Similarly, here it is implicitly assumed that there is a single owner of all of the facilities involved (or, at least, that the owners fully cooperate and behave as such). However, those facilities can belong to different owners. In this case, if the whole infrastructure is to be assembled, it can be essential to design a fair or reasonable profit allocation rule; Wang *et al.* [49]. Again, this paper does not address this issue.

On the other hand, a number of parameter values are assumed to remain fixed over 30 years. Since the technology for producing hydrogen from RES via electrolysis is in its infancy, this assumption is especially restrictive; think, for instance, of conversion efficiencies and facilities' costs. As the technology diffusion leaves the formative phase behind, market adoption will accelerate thanks to learning effects and returns to scale (thus entering the so—called growth phase). In principle, it is possible to perform a sensitivity analysis with respect to any one underlying variable. However, when it comes to green hydrogen, players actually face a threefold coordination challenge: simultaneously ramping up hydrogen supply, end-use applications (i.e. demand), and transport infrastructure; Odenweller *et al.* [50]. This study refrains from following this broader approach (which calls for going beyond sensitivity analysis) and instead restricts itself to a narrower one.

Similarly, the authors neglect the potential systemic impacts of adding hydrogen electrolyzers to the energy system. Thus, Green *et al.* [46] find that their large-scale adoption will raise the average price of electricity and change the optimal mix of power stations. In this sense, the authors perform a partial equilibrium analysis. Further, the word 'system' can be pushed to a higher level, namely by considering cross-border transmission interconnections. In our case, the Iberian peninsula continues to be an 'electric island' to some extent; Abadie and Chamorro [22]. In principle, isolated systems with (relatively) high wind penetration need additional backup capacity for long periods (when the wind does not blow) than systems that benefit from strong interconnectors. Consequently, all else equal, the cost of hydrogen will be higher in systems like Spain; Greiner *et al.* [51], Korpas and Greiner

[52].

Some venues for future research include: (1) the impact of increased spot power prices since the spring of 2021 on the production of green hydrogen in the short term; (2) the analysis of this impact on a cross section of countries (Spain, France, Germany, Italy, Belgium, and the Netherlands); (3) the impact of futures electricity prices on the production of green hydrogen in the long term; (4) extending the model with additional stochastic variables, e.g. curtailment rate; (5) extending the model with an additional industrial facility, e.g. a steel mill, or a cement producer; (6) analysis of the effect of changes in alternative policy measures to support the development of the hydrogen economy.

Declaration of Competing Interest

The authors declare that they have no known competing financial interests or personal relationships that could have appeared to influence the work reported in this paper.

Data availability

Data will be made available on request.

Data availability.

The authors have drawn on the database of the Spanish power transmission and distribution system operator (Red Eléctrica de España), which is publicly available: https://www.esios.ree.es/

Appendix A

This section explains the process behind the particular value of wind energy's curtailment rate, namely 7.74 %. The authors draw on Yasuda *et al*. (2022), "*Table 1: Statistical data for wind curtailment in European countries*". The authors collect the data of "*Energy share of wind in a given country/area [%]*" and "*Curtailment ratio of wind energy in a given country/area [%]*" wherever both series are available (Denmark, Germany, Northern Ireland, Italy, Spain and UK) over the period 2009–2020 (in total, 65 observations). See Fig. A1.

Next, the authors estimate a linear regression model with the curtailment ratio as independent variable. An obvious assumption is that the straight line starts from the origin. The outcome is:

Curtailment ratio $= 0.154797 \times$ *Wind share*

Though not shown here, sample data suggest similar shares of wind energy in several countries, e.g. Germany, Spain and the U.K., about 25 % in 2020. The authors anticipate that this share will increase further in the future. Looking far ahead, a share of 50 % implies a curtailment ratio of 7.74 %, the level used in our above calculations. The authors undertake a sensitivity analysis in Section 6.2.

Appendix B

Fig. B.1 shows the evolution of onshore wind farms installed capacity in the four years.

Fig. B.1 suggests three different deployment phases. The longest one is the initial period, when wind capacity barely increases. The second one goes from summer 2018 to summer 2019, and is characterized by a consistent, mild growth. Yet, it is in the last four months of 2018 that capacity sharply rises.

Appendix C

Table A2

References

[1] International Energy Agency. Net zero by 2050: A roadmap for the global energy sector. 2021. https://www.iea.org/reports/net-zero-by-2050.

[2] Sinsel SR, Riemke RL, Hoffmann VH. Challenges and solution technologies for the integration of variable renewable energy sources-a review. Renew Energy 2020; 145:2271–85. https://doi.org/10.1016/j.renene.2019.06.147.

[3] Nikolaidis P, Poullikkas A. A comparative overview of hydrogen production processes. Renew. Sustainable Energy Rev. 2017;67:597–611. https://doi.org/10.1016/j.rser.2016.09.044.

[4] Stöckl F, Schill WP, Zerrahn A. Optimal supply chains and power sector benefits of green hydrogen. Nat. Portfolio, Scientific Rep. 2021;11:14191. https://doi.org/10.1038/s41598-021-92511-6.

[5] Gahleitner G. Hydrogen from renewable electricity: an international review of power-to-gas pilot plants for stationary applications. Int J Hydrogen Energy 2013; 38:2039–61. https://doi.org/10.1016/j.ijhydene.2012.12.010.

[6] Jaunatre M. Renewable Hydrogen. Springer Gabler: Business Analytics; 2021.

[7] Schultes G, Madlener R. Investment under uncertainty in a power-to-gas plant in Germany: a Real Options Analysis. Mimeo; 2020.

[8] Glenk G, Reichelstein S. Economics of converting renewable power to hydrogen. Nat Energy 2019;4:216–22. https://doi.org/10.1038/s41560-019-0326-1.

[9] Shaner MR, Atwater HA, Lewis NS, McFarland EWA. comparative techno-economic analysis of renewable hydrogen production using solar energy. Energ Environ Sci 2016;9:2354–71. https://doi.org/10.1039/c5ee02573g.

[10] Way R, Ives MC, Mealy P, Farmer JD. Empirically grounded technology forecasts and the energy transition. Joule 2022;6:1–26. https://doi.org/10.1016/j.joule.2022.08.009.

[11] Touili S, Merrouni AA, Azozoute A, El Hassaouani Y, Amrani A. A technical and economical assessment of hydrogen production potential from solar energy in Morocco. Int J Hydrogen Energy 2018;43:22777–96. https://doi.org/10.1016/j.ijhydene.2018.10.136.

[12] van Benthem AA, Kramer GJ, Ramer R. An options approach to investment in a hydrogen infrastructure. Energy Policy 2006;34:2949–63.

[13] Guerra OJ, Eichman J, Kurtz J, Hodge B-M. Cost Competitiveness of Electrolytic Hydrogen Joule 2019;3:2425–43. https://doi.org/10.1016/j.joule.2019.07.006.

[14] Talebian H, Herrera OE, Mérida W. Policy effectiveness on emissions and cost reduction for hydrogen supply chains: the case for British Columbia. Int J Hydrogen Energy 2021;46:998–1011. https://doi.org/10.1016/j.ijhydene.2020.09.190.

[15] Coppitters D, Verleysen K, De Paepe W, Contino F. How can renewable hydrogen compete with diesel in public transport? Robust design optimization of a hydrogen refueling station under techno-economic and environmental uncertainty. Appl Energy 2022;312:118694. https://doi.org/10.1016/j.apenergy.2022.118694.

[16] Isaqh H, Dincer I, Naterer GF. Performance investigation of an integrated wind energy system for co-generation of power and hydrogen. Int J Hydrogen Energy 2018;43:9153–64. https://doi.org/10.1016/j.ijhydene.2018.03.139.

[17] Farhat K, Reichelstein S. Economic value of flexible hydrogen-based polygeneration energy systems. Appl Energy 2016;164:857–70. https://doi.org/10.1016/j.apenergy.2015.12.008.

[18] Klyapovskiy S, Zheng Y, You S, Bindner HW. Optimal operation of the hydrogen-based energy management system with P2X demand response and ammonia plant. Appl Energy 2021;304:117559. https://doi.org/10.1016/j.apenergy.2021.117559.

[19] Kroniger D, Madlener R. Hydrogen storage for wind parks: a real options evaluation for an optimal investment in more flexibility. Appl Energy 2014;136:931–46. https://doi.org/10.1016/j.apenergy.2014.04.041.

[20] Grueger F, Möhrke F, Robinius M, Stolten D. Reducing wind farm forecast errors and providing secondary control reserve. Appl Energy 2017;192:551–62. https://doi.org/10.1016/j.apenergy.2016.06.131.

[21] Eypasch M, Schimpe M, Kanwar A, Hartmann T, Herzog S, Frank T, et al. Model-based techno-economic evaluation of an electricity storage system based on Liquid Organic Hydrogen Carriers. Appl Energy 2017;185:320–30. https://doi.org/10.1016/j.apenergy.2016.10.068.

[22] Abadie LMª, Chamorro JM. Evaluation of a cross-border electricity interconnection: the case of Spain-France. Energy 2021;233:121177. https://doi.org/10.1016/j.energy.2021.121177.

[23] Reichelstein S, Sahoo A. Time of day pricing and the levelized cost of intermittent power generation. Energy Econ 2015;48:97–108. https://doi.org/10.1016/j.eneco.2014.12.005.

[24] Red Eléctrica de España. https://www.esios.ree.es/.

[25] International Energy Agency. Projected costs of generating technologies. 2020 Edition.

[26] Han S, He M, Zhao Z, Chen D, Xu B, Jurasz J, Liu F, Zheng H. Overcoming the uncertainty and volatility of wind power: Day-ahead scheduling of hydro-wind hybrid power generation system by coordinating power regulation and frequency response flexibility. Applied Energy 2023;333:120555. Doi: 10.1016/j.apenergy.2022.120555.

[27] Isaqh H, Dincer I. Dynamic analysis of a new solar-wind energy-based cascaded system for hydrogen to ammonia. Int J Hydrogen Energy 2020;45:18895–911. https://doi.org/10.1016/j.ijhydene.2020.04.149.

[28] Fripp M, Wiser RH. Effects of temporal wind patterns on the value of wind-generated electricity in california and the northwest. IEEE Trans Power Syst 2008;23(2):477–85. https://doi.org/10.1109/TPWRS.2008.919427.

[29] Jørgensen C, Ropenus S. Production price of hydrogen from grid connected electrolysis in a power market with high wind penetration". Int J Hydrogen Energy 2008;33(20):5335–44.

[30] Reuter WH, Szolgayová J, Fuss S, Obersteiner M. Renewable energy investment: policy and market impacts. Appl Energy 2012;97:249–54. https://doi.org/10.1016/j.apenergy.2012.01.021.

[31] Zheng Y, Wang J, You S, Li X, Bindner HW, Münster M. Data-driven scheme for optimal day-ahead operation of a wind/hydrogen system under multiple uncertainties. Appl Energy 2023;329:120201. https://doi.org/10.1016/j.apenergy.2022.120201.

[32] Çanakoğlu E, Adıyeke E. Comparison of electricity spot price modelling and risk management applications. Energies 2020;13(18):4698. https://doi.org/10.3390/en13184698.

[33] Staffell I, Green R. How does wind farm performance decline with age? Renew Energy 2014;66:775–86. https://doi.org/10.1016/j.renene.2013.10.041.

[34] Mohsin M, Rasheed AK, Saidur R. Economic viability and production capacity of wind generated renewable hydrogen. Int J Hydrogen Energy 2018;43:2621–30. https://doi.org/10.1016/j.ijhydene.2017.12.113.

[35] Joos M, Staffell I. Short-term integration costs of variable renewable energy: wind curtailment and balancing in Britain and Germany. Renew Sustain Energy Rev 2018;86:45–65. https://doi.org/10.1016/j.rser.2018.01.009.

[36] Steurer M, Fahl U, Voss A, Deane P. Curtailment: an option for cost-efficient integration of variable renewable generation? In: Europe's Energy Transition, Elsevier 2017:97–104. https://doi.org/10.1016/B978-0-12-809806-6.00015-8.

[37] Yasuda Y, Bird L, Carlini EM, Eriksen PB, Estanqueiro A, Flynn D et al. C-E (curtailment – energy share) map: An objective and quantitative measure to evaluate wind and solar curtailment. Renewable and Sustainable Energy Reviews 2022;160:112212, 1–14. Doi: 10.1016/j.rser.2022.112212.

[38] Bird L, Lew D, Milligan M, Carlini EM, Estanqueiro A, Flynn D, et al. Wind and solar energy curtailment: a review of international experience. Renew Sustain Energy Rev 2016;65:577–86. https://doi.org/10.1016/j.rser.2016.06.082.

[39] IRENA. Renewable Power Generation Costs in 2020. International Renewable Energy Agency 2022, Abu Dhabi. ISBN 978-92-9260-348-9.

[40] Armijo J, Philibert C. Flexible production of green hydrogen and ammonia from variable solar and wind energy: Case study of Chile and Argentina. Int J Hydrogen Energy 2020;45:1541–58. https://doi.org/10.1016/j.ijhydene.2019.11.028.

[41] Newey WK, West KD. A simple, positive semi-definite, heteroskedasticity and autocorrelation consistent covariance matrix. Econometrica 1987;55:703–8. https://doi.org/10.2307/1913610.

[42] Long JS. Regression models for categorical and limited dependent variables. SAGE Publications; 1997.

[43] Duan L, Petroski R, Wood L, Caldeira K. Stylized least-cost analysis of flexible nuclear power in deeply decarbonized electricity systems considering wind and solar resources worldwide. Nat Energy 2022;7:260–9. https://doi.org/10.1038/s41560-022-00979-x.

[44] IRENA. Future of Wind. Deployment, investment, technology, grid integration and socio-economic aspects. (A Global Energy Transformation paper). International Renewable Energy Agency 2019, Abu Dhabi. ISBN 978-92-9260-155-3.

[45] Aguado M, Ayerbe E, Azcárate C, Blanco R, Garde R, Mallor F, et al. Economical assessment of a wind-hydrogen energy system using WindHyGen® software. Int J Hydrogen Energy 2009;34:2845–54. https://doi.org/10.1016/j.ijhydene.2008.12.098.

[46] Green R, Hu H, Vasilakos N. Turning the wind into hydrogen: The long-run impact on electricity prices and generating capacity. Energy Policy 2011;39:3992–8. https://doi.org/10.1016/j.enpol.2010.11.007.

[47] Steffen B. Estimating the cost of capital for renewable energy projects. Energy Econ 2020;88(104783):1–14. https://doi.org/10.1016/j.eneco.2020.104783.

[48] Hosseini SE, Wahid MA. Hydrogen production from renewable and sustainable energy resources. Renew Sustain Energy Rev 2016;57:850–66. https://doi.org/10.1016/j.rser.2015.12.112.

[49] Wang X, Li B, Wang W, Lu H, Zhao H, Xue W. A bargaining game-based profit allocation method for the wind-hydrogen-storage combined system. Appl Energy 2022;310:118472. https://doi.org/10.1016/j.apenergy.2021.118472.

[50] Odenweller A, Ueckerdt F, Nemet GF, Jensterle M, Luderer G. Probabilistic feasibility space of scaling up green hydrogen supply. Nat Energy 2022;7:854–65. https://doi.org/10.1038/s41560-022-01097-4.

[51] Greiner CJ, Korpas M, Holen AT. A Norwegian case study on the production of hydrogen from wind power. Int J Hydrogen Energy 2007;32:1500–7.

[52] Korpas M, Greiner CJ. Opportunities for hydrogen production in connection with wind power in weak grids. Renew Energy 2008;33(6):1199–208.